

Keep Paper Copy

DoE

EPA

United States
Department
of Energy

Fossil Energy Division
Fossil Fuel Utilization
Washington DC 20540

ANL/CEN/FE-78-13

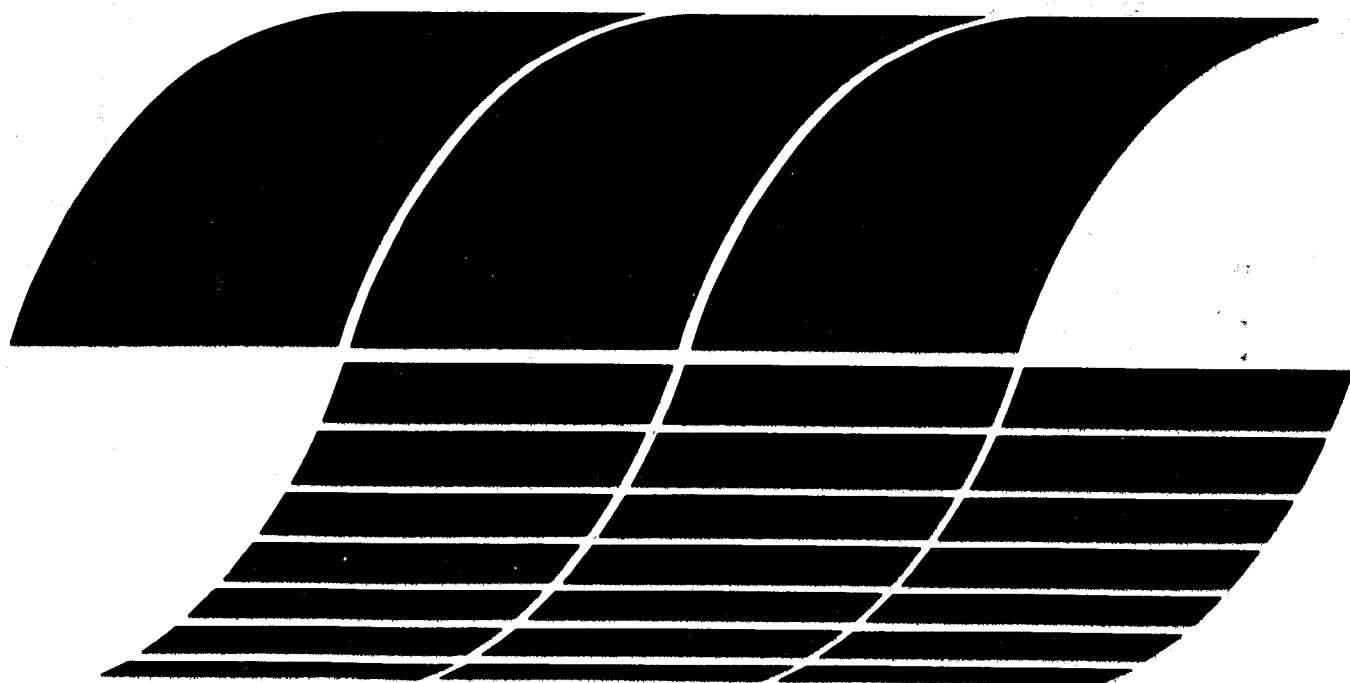
United States Environmental
Protection Agency
Office of Research and Development

Industrial Environmental Research
Laboratory
Research Triangle Park NC 27711

EPA-600/7-79-157
July 1979

Regeneration of Sulfated Limestone from FBCs and Corrosive Effects of Sulfation Accelerators in FBCs: Annual Report

**Interagency
Energy/Environment
R&D Program Report**



RESEARCH REPORTING SERIES

Research reports of the Office of Research and Development, U.S. Environmental Protection Agency, have been grouped into nine series. These nine broad categories were established to facilitate further development and application of environmental technology. Elimination of traditional grouping was consciously planned to foster technology transfer and a maximum interface in related fields. The nine series are:

1. Environmental Health Effects Research
2. Environmental Protection Technology
3. Ecological Research
4. Environmental Monitoring
5. Socioeconomic Environmental Studies
6. Scientific and Technical Assessment Reports (STAR)
7. Interagency Energy-Environment Research and Development
8. "Special" Reports
9. Miscellaneous Reports

This report has been assigned to the INTERAGENCY ENERGY-ENVIRONMENT RESEARCH AND DEVELOPMENT series. Reports in this series result from the effort funded under the 17-agency Federal Energy/Environment Research and Development Program. These studies relate to EPA's mission to protect the public health and welfare from adverse effects of pollutants associated with energy systems. The goal of the Program is to assure the rapid development of domestic energy supplies in an environmentally-compatible manner by providing the necessary environmental data and control technology. Investigations include analyses of the transport of energy-related pollutants and their health and ecological effects; assessments of, and development of, control technologies for energy systems; and integrated assessments of a wide range of energy-related environmental issues.

EPA REVIEW NOTICE

This report has been reviewed by the participating Federal Agencies, and approved for publication. Approval does not signify that the contents necessarily reflect the views and policies of the Government, nor does mention of trade names or commercial products constitute endorsement or recommendation for use.

This document is available to the public through the National Technical Information Service, Springfield, Virginia 22161.

Regeneration of Sulfated Limestone from FBCs and Corrosive Effects of Sulfation Accelerators in FBCs: Annual Report

by

G. J. Vogel, I. Johnson, J. F. Lenc, D. S. Moulton,
R. B. Snyder, J. A. Shearer, G. W. Smith, W. M. Swift,
E. B. Smyk, F. G. Teats, C. B. Turner, and A. A. Jonke

Argonne National Laboratory
9700 South Cass Avenue
Argonne, Illinois 60439

EPA No. IAG-D5-E681
DoE No. W-31-109-Eng-38
Program Element No. INE825

Project Officers:

David A. Kirchgessner
EPA/Industrial Environmental
Research Laboratory
Research Triangle Park, NC 27711

John F. Geffken
DoE/Fossil Fuel Utilization
Washington, DC 20540

Prepared for

U.S. ENVIRONMENTAL PROTECTION AGENCY
Office of Research and Development
Washington, DC 20460

U.S. DEPARTMENT OF ENERGY
Fossil Fuel Utilization
Washington, DC 20540

TABLE OF CONTENTS

	<u>Page</u>
ABSTRACT	1
SUMMARY	1
TASK A. REDUCTIVE DECOMPOSITION PROCESS STUDIES	3
1. Experimental Studies	3
2. Prediction of Process Parameters Based on a Regeneration Model	5
3. Predicted Effects of Off-Design Conditions on Regenerator Operating Parameters	19
4. Comparison of New and Earlier Predictions of Effects of Process Parameters	24
5. Economic Feasibility of Regenerating Sulfated Limestone	27
TASK B. ALTERNATIVE REGENERATION PROCESS DEVELOPMENT	28
1. Rotary-Kiln Regeneration	28
TASK D. EFFECTS OF LIMESTONE SULFATION ACCELERATORS ON CORROSION RATES OF METALS IN AN AFBC	34
1. Atmospheric Combustor Facility for Corrosion Tests	34
2. Corrosion Behavior of Materials in Fluidized-Bed Environments	42
REFERENCES	62

LIST OF FIGURES

<u>No.</u>	<u>Title</u>	<u>Page</u>
1.	Flow Sheet for Conceptual 635-MW Atmospheric Fluidized-Bed Combustor	6
2.	Velocity Ratio <u>vs.</u> Inclination Angle in a Laboratory-Scale Rotary Kiln	30
3.	Gas-Sampling Locations and Reactor Temperatures in the Laboratory-Scale Rotary Kiln Operated at 1040°C and 4 rpm	31
4.	Variation of Percent SO ₂ in Off-Gas with Carrier-Gas Flow Rate, during Limestone Regeneration in a Small Rotary Kiln at 1040°C	32
5.	Simplified Piping Schematic of Atmospheric Combustor Facility	35
6.	152-mm-ID Atmospheric Combustor	36
7.	Some Major Components of the New AFBC	37
8.	Automatic Control Loops for Atmospheric Combustor Facility	39
9.	High-Temperature 5-cm-dia Quartz Fluidized-Bed Reactor for Salt Corrosion Studies	43
10.	Average Thickness of Surface Scale and Corrosive Penetration for Corrosion Coupons Exposed Inside the Bed for 100 h at 1123 K except that the Temperature for Inconel 601 was 1173 K	45
11.	Average Thickness of Surface Scale and Corrosive Penetration for Corrosion Coupons Exposed Above the Bed for 100 h at 1123 K except that for Inconel 601 the Temperature was 1173 K	46
12.	SEMs of Type 304 Stainless Steel after a 100-h Exposure at 1123 K	47
13.	SEMs of Type 310 Stainless Steel after a 100-h Exposure at 1123 K	48
14.	SEMs of Incoloy 800 after a 100-h Exposure at 1123 K	49
15.	SEMs of Inconel 600 after a 100-h Exposure at 1123 K	50
16.	SEMs of Inconel 601 after a 100-h Exposure at 1123 K	51
17.	SEMs of RA333 after a 100-h Exposure at 1123 K	52
18.	X-ray Microprobe Line Analyses for Ni, Fe, and Cr on Incoloy 800 Specimens Exposed above the Bed for 100 h at 1123 K	53

LIST OF FIGURES (contd)

<u>No.</u>	<u>Title</u>	<u>Page</u>
19.	SEMs and EDAX Analysis of the Surface of the Scales Developed on Incoloy 800 Exposed above the Bed for 100 h at 1123 K	54
20.	SEMs of Type 304 Stainless Steel after a 100-h Exposure	56
21.	SEMs of Type 310 Stainless Steel after a 100-h Exposure	57
22.	X-ray Microprobe Line Analyses for Fe, Cr, Ni, O, and S on Type 304 Stainless Steel Specimen Exposed Above the Bed Containing NaCl for 100 h at 923 K	59
23.	SEMs and X-ray Images for Fe, Cr, O, S, and Cl of Type 304 Stainless Steel Specimen Exposed Above the Bed Containing NaCl for 100 h at 923 K	60
24.	SEMs of (a) Sulfide/Mixed-Oxide Interface and (b) Mixed-Oxide/Iron-Oxide Interface Observed in Type 304 Stainless Steel Specimen Exposed Above the Bed for 100 h at 823 K	61

LIST OF TABLES

<u>No.</u>	<u>Title</u>	<u>Page</u>
1.	Baseline Conditions for Flow Sheet	7
2.	Predicted Effects of Feed Ratio on Regeneration System Performance and Dimensions	8
3.	Predicted Effects of Superficial Gas Velocity on Regenerator Dimensions	10
4.	Predicted Effects of Solids Residence Time on Regenerator Dimensions and Performance	11
5.	Predicted Effects of Solids Feed Temperature and Gas Inlet Temperature on Regenerator Dimensions and Performance	13
6.	Predicted Effects of Regenerator Bed Temperature on Regenerator Dimensions and Performance	15
7.	Predicted Effect of Pressure on Regenerator Dimensions	17
8.	Predicted Effect of Changes in Feed-Gas Oxygen Concentration on Regenerator Dimensions and Performance	18
9.	Predicted Effects of Off-Design Conditions on Regenerator Performance	20
10.	Design of Regenerator to Accommodate Turndown	23
11.	Regeneration of Sulfated Greer Limestone with Char in a Small Rotary Kiln	31
12.	Regeneration at 1040°C of Spent Limestone Sorbent in a Small Rotary Kiln	33
13.	Nominal Operating Conditions. Atmospheric Fluidized-Bed Combustor	38
14.	Control Loops for Atmospheric Fluidized-Bed Combustor	40
15.	Process Levels Necessitating Shutdown	41
16.	Compositions of Alloys	43
17.	Experimental Conditions	44

REGENERATION OF SULFATED LIMESTONE FROM FBCs AND
CORROSIVE EFFECTS OF SULFATION ACCELERATORS IN FBCs
ANNUAL REPORT

July 1977 - September 1978

by

G. J. Vogel, Irving Johnson, O. K. Chopra, J. F. Lenc,
D. S. Moulton, J. A. Shearer, R. B. Snyder,
G. W. Smith, W. M. Swift, E. B. Smyk,
F. G. Teats, C. B. Turner, and A. A. Jonke

ABSTRACT

These studies support the national development program in fluidized-bed combustion. The objectives of this program are to develop an economically and environmentally acceptable process for the regeneration of the partly sulfated product of a fluidized-bed coal combustor, to obtain the design data needed for the construction of larger regenerators, and to determine the possible corrosive effect on metallic alloys of sulfation acceleration agents added to the limestone sorbent. A regeneration process model has been developed; the model has been used to investigate the effects of the main variables on regenerator size and performance and to estimate the economic feasibility of regeneration. The results of an investigation of a regeneration process using a rotary kiln in place of a fluidized bed are reported. An atmospheric pressure FBC was placed into operation to study the corrosion of metallic alloys by limestone treated with various sulfation accelerators such as NaCl or CaCl₂. The results of corrosion studies carried out in a laboratory-scale facility are reported.

SUMMARY

Task A. Reductive Decomposition Process Studies

Experimental. Work continued on characterization of the reductive decomposition of sulfated limestone in a coal-fired fluidized-bed regenerator. Three experimental studies were done in the ANL 10.8-cm-ID bench-scale unit: (1) to ascertain the effect of preheating sorbent feed to the regenerator, (2) to ascertain the effect of high bed temperature on extent of regeneration, and (3) to determine if hot spots are present in the regenerator bed near the coal feed point.

The regeneration model correctly predicted the effect of solids preheat, although SO₂ enrichment in the off-gas was not obtained because of the experimental procedure. A high temperature (1423 K vs. 1373 K) in the regenerator resulted in a small increase in the extent of regeneration of CaO.

However, defluidization velocity was about 40% higher than at 1373 K. No hot spots were detected in the regenerator bed near the coal feed points.

Development of a Regeneration Process Model. On the basis of experimental results obtained in the ANL 10.8-cm-ID bench-scale fluidized-bed regenerator, a mass- and energy-balance constrained model for the reductive decomposition of sulfated limestone has been developed. The model allows regenerator performance and dimensions to be predicted, given specific operating conditions. Results are presented for the effects of feed ratio (FR), superficial gas velocity, solids residence time, gas and solids feed temperatures, bed temperature and pressure, and feed-gas oxygen concentration on regenerator performance and dimensions. The effect of off-design conditions on (1) regenerator operating parameters and (2) methods of designing a regenerator to accommodate turndown are discussed. Finally, methods of interpreting process development unit (PDU) experimental data for use in designing larger regenerators are presented.

Economic Feasibility of Regenerating Sulfated Limestone. An economic analysis of regenerator and sulfur-recovery systems was done to determine which factors were important and to what degree. Capital cost, capacity factor, and sorbent price (including disposal cost) were found to be important factors, while fuel price and sulfur credit value were found to be of lesser importance.

Task B. Alternative Regeneration Process Development

Rotary Kiln Regeneration. Rotary kilns are being evaluated as an alternative to fluidized-bed reactors for the regeneration of sulfated limestone. Studies are being conducted in a laboratory-scale rotary kiln to demonstrate the process and to obtain data for larger-scale tests. Tests made using sulfated Greer limestone mixed with coal char at 1040°C indicated that SO₂ concentrations near the equilibrium value of 20% can be obtained. Regenerations of about 40% of the CaSO₄ were obtained.

Task D. Effects of Limestone Sulfation Accelerators on Corrosion Rates of Metals in an AFBC

Atmospheric Combustor Facility for Corrosion Tests. A new PDU-scale automated atmospheric-pressure fluidized-bed coal combustion facility (AFBC) was constructed. The facility will be used in an experimental program to study the corrosive effects on metals of construction of agents (e.g., NaCl, CaCl₂, or Na₂CO₃) that accelerate limestone sulfation. The new facility, including the process-control system for automated operation, is described.

A series of runs is being carried out in the new AFBC (prior to corrosion experiments) to evaluate the effects on SO₂ retention of adding low concentrations (1.0 mol % or less) of CaCl₂ or NaCl to Grove limestone. A total of 31 runs in this series have been conducted. Evaluation of the results awaits the completion of analyses.

Compositions and geometries of corrosion specimens, as well as locations of exposure, have been selected. Parameters to be measured during corrosion tests have been identified.

To obtain baseline corrosion data on a variety of metals, initial corrosion combustion experiments are to be conducted with no sulfation accelerator present in the fluidized bed. Next, 100-h scoping tests will be made to determine the effects of sulfation accelerators on corrosion specimens of various metals. Following the 100-h tests, those metals and accelerating agents selected for further testing will be subjected to 1000-h tests.

Corrosion Behavior of Materials in Fluidized-Bed Environment. As part of the study of the effect of NaCl and other salts on the utilization of limestone for SO₂ absorption in FBCs, a series of corrosion tests were made in a laboratory-scale fluidized-bed reactor. These tests were done with a gas mixture containing from 200 to 500 ppm SO₂, 5% O₂, and the rest N₂. In the tests, at 850°C and of 100-h duration, samples were exposed within or above the fluidized bed of sulfated dolomite. Tests were done with salt present in or absent from the bed.

Metallographic examination of the samples indicated (1) the addition of NaCl or CaCl₂ to the bed increases corrosion; (2) in the presence of salt, Types 304, 316, and 310 stainless steel perform better than did high-nickel alloys; (3) the corrosion behavior of stainless steels is relatively insensitive to the NaCl concentration in the bed; (4) the corrosion behavior of Inconel 600, Inconel 601, and RA333 in the presence of 1 mol % NaCl or 0.1 mol % CaCl₂ is comparable to that of the stainless steels; (5) the internal corrosive attack consists of three distinct zones: internal oxidation, internal sulfidation, and a carburized zone; and (6) specimens exposed above the bed at 923 and 823 K show extensive corrosive attack.

TASK A. REDUCTIVE DECOMPOSITION PROCESS STUDIES (E. B. Smyk and R. B. Snyder)

1. Experimental Studies

A fluidized-bed reductive decomposition process for regenerating lime from partially sulfated limestone, using coal as both a reductant and a heat source, has been developed in a 10.8-cm-ID regenerator. In earlier work,^{1,2} experiments were performed to ascertain the effects of bed temperature, solids residence time (SRT), superficial gas velocity, feed-gas oxygen concentration, and bed height on process performance (most notably, off-gas SO₂ concentration).

In all earlier regeneration experiments at ANL, room-temperature sulfated sorbent was fed to the regenerator reactor. In an industrial process, the sorbent would enter the reactor at about 1116 K. The effect of sorbent feed temperature on CaO regeneration has been tested. Experiments were performed with 600-2000 μm (-10 +30 mesh) and 600-1400 μm (-14 +30 mesh) sulfated Greer limestone from Pope, Evans, and Robbins (PER) with sorbent preheating temperatures of 1075-1175 K. Preheating the solids feed permitted experiments to be done in the ANL 10.8-cm-ID reactor with solids residence times (SRTs) as brief as 4.4 min. (The range of SRTs was about 4 to 10 min.) In earlier experimental work, all regeneration experiments were performed with SRTs greater than 7 min.

In the regeneration experiments with the larger sulfated limestone particles (600-2000 μm), the extent of regeneration at a high SRT was equivalent to that projected from previous experiments² with finer (600-1400 μm) limestone. However, even with feed sorbent preheated to 1150 K at a relatively low SRT (5.4 min), the extent of regeneration was lower than that projected for large particles. Because regeneration reactions are relatively rapid, it is believed that the lower conversion could be due to poorer fluidization of the larger particles in the rather small reactor.

In the experiments with small sulfated limestone particulate (600-1400 μm), preheating the solids feed (>1150 K) was beneficial. The extent of regeneration for SRTs as low as 4.4 min were equivalent to the projections made from previous experiments performed at higher SRTs (>7 min). Preheating the solids improved the extent of regeneration at the lower SRTs (<7 min) and allowed it to reach the predicted values. The SO_2 concentration in the off-gas generally increased from 6% to 10.4% as the SRT was decreased; this was expected.

In these experiments, as predicted from the regeneration process model,² solids preheat did not cause SO_2 enrichment because of the way regeneration experiments are performed at ANL-- O_2 and N_2 are mixed to satisfy the oxygen demand of the reactor while a constant total gas input is maintained. Changes in gas velocity in these experiments are thereby avoided. Therefore, the SO_2 concentrations obtained in these experiments are equivalent to those expected in an industrial process in which the solids would be fed hot to the regenerator reactor.

The effect of a regeneration temperature in excess of 1373 K was tested by performing a regeneration and defluidization experiment at 1423 K. This is the highest temperature at which a regeneration experiment has been performed at ANL. Regeneration was not significantly greater than that obtained at 1373 K. Moreover, the higher temperature caused a drastic increase (about 40%) in the defluidization velocity (the minimum gas velocity required to prevent agglomeration). The net effect of this and the very small increase in the extent of regeneration is a lower SO_2 concentration in the regeneration reactor off-gas. Also, higher temperatures accelerate the sintering process, rendering the sorbent less reactive in subsequent sulfation steps. Therefore, temperatures higher than 1373 K do not seem to offer improved performance in the regeneration step of an FBC process.

In multicyclic usage of sorbent, loss of sorbent reactivity could be greater than normal due to localized high-temperature spots near the coal feed point. The regenerator bed temperature near the coal feed point was measured with a probe to evaluate the extent of any such hot spots. The local temperature 2.5 to 9.2 cm from the coal injection point along the jet path was found to exceed other bed-temperature measurements by not more than 5 degrees K. More detailed results have been previously reported.¹

2. Prediction of Process Parameters Based on a Regeneration Model

Experimental development of the fluid-bed, reductive decomposition regeneration process for partially sulfated limestone, using a PDU regenerator, has been successful. The regenerator is 10.8 cm in ID, and the expanded bed height is 45 cm. The extent of regeneration of the partially sulfated limestone and the SO_2 concentration in the off-gas were determined as a function of various operating conditions. These results were reported previously.²

Here, a process flow sheet is discussed for a conceptual 635-MW FBC process with sorbent regeneration, using Greer limestone. The performance of Greer limestone as a function of cycle number was established in a ten-cycle experiment,³ and the results pertaining to reactivity, calcium utilization, ash buildup, and elutriation as a function of cycle number have been incorporated into the ANL-developed regeneration process model. Results presented here differ somewhat from previous ones since the regeneration model has been made rigorous and all material balances have been closed.

Figure 1 presents a process flow sheet for a 635-MW AFBC burning Sewickley coal and utilizing Greer limestone as the sorbent, coupled to a regenerator and sulfur-recovery system. The baseline conditions are presented in Table 1; these are typical but not necessarily optimum. The sulfated limestone is assumed to be introduced into the regenerator at 1116 K (1550°F), which is the bed temperature in the fluid-bed combustor. The superficial gas velocity of 1.4 m/s is 12% above the velocity predicted to be necessary to prevent agglomeration (and consequently defluidization) for sorbent particles having a mean size of 1500 μm ($-1/8$ in.) when regenerated at 1373 K with 2% total reducing gas in the regenerator off-gas. The feed gas to the regenerator is assumed to be heated to 675 K by recovering waste heat from the regenerator off-gas.

The coal consumption of the total regenerator system with 1116 K solid and 675 K gas feed streams was estimated to be 95 Mg/d. The fuel consumption of the total regeneration system is obtained by adding the coal fed to the regenerator (178 Mg/d) to the coal fed to the sulfur-recovery step (47 Mg/d) and subtracting the fuel credits for the regenerator off-gas cyclone product (51 Mg/d) and the sensible heats of (1) the regenerated sorbent (41 Mg/d) and (2) the tail-gas stream from the sulfur-recovery step (38 Mg/d) that will be recycled to the boiler.

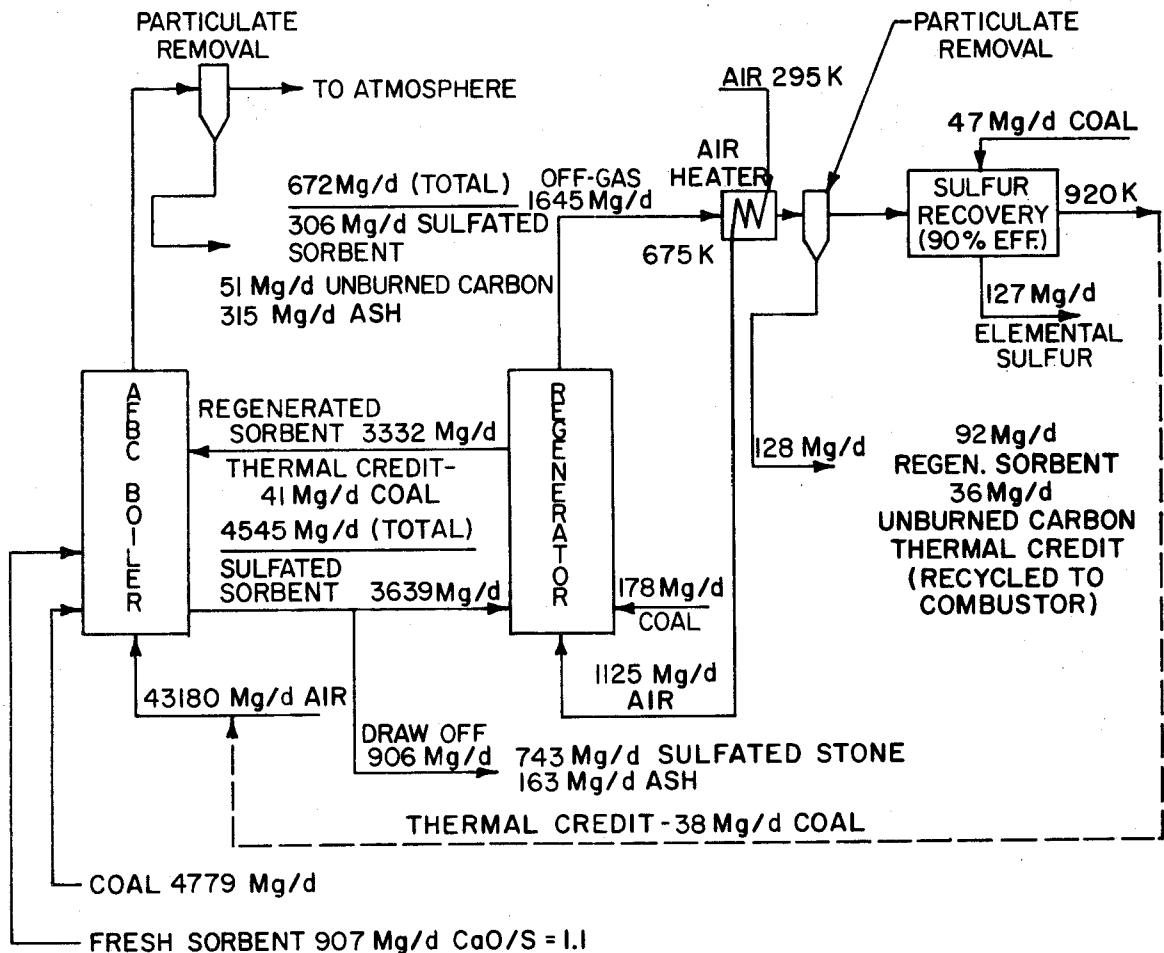


Fig. 1. Flow Sheet for Conceptual 635-MW Atmospheric Fluidized-Bed Combustor. Fresh sorbent feed CaO/S ratio = 1.1.

a. Predicted Effect of Feed Ratio on Regenerator Dimensions and Performance

Once the sulfur content of the coal is given, the SO₂ retention necessary to meet EPA emission regulations can be calculated. Based on the reactivity of a given stone, the CaO/S mole ratio necessary to provide the needed SO₂ retention can be projected. Tests in which the sorbent was repeatedly cycled between the combustor and regenerator have shown that the sorbent has less reactivity at higher regeneration-cycle numbers. It is thus possible to predict the CaO/S mole ratio necessary to provide the necessary SO₂ retention as a function of regeneration-cycle number. Feed ratio (FR) is defined as the amount of CaO in the fresh feed, divided by the total CaO fed to the combustor. The process model allows the overall CaO/S ratios needed for SO₂ retention to be predicted as a function of FR by calculating the age (regeneration-cycle number) distribution of regenerated sorbent as a function of FR and adding the resulting reactivity to the reactivity of the fresh sorbent.

Table 1. Baseline Conditions for Flow Sheet (Fig. 1)

<u>Coal</u>	<u>Sorbent</u>
Sewickley coal	Greer limestone
28.5 MJ/kg (12250 Btu/lb)	80% CaCO ₃
4.3% S	20% Inert
10.0% Ash	
<u>AFBC Boiler</u>	
635 MW at 37% conversion efficiency (9200 Btu/kW·h)	
Bed Temperature - 1116 K (1550°F)	
Pressure - 103 kPa (1 atm)	
Bed Area - 767 m ² (8255 ft ²)	
Combustion Efficiency - 99%	
Sulfur Retention - 83%	
Fresh/Total Sorbent Feed Ratio (FR) ^a - 0.2	
<u>Regenerator</u>	
Bed Temperature - 1373 K (2012°F)	
Pressure - 103 kPa (1 atm)	
Bed Area - 36.2 m ² (389 ft ²)	
Bed Height - 0.67 m (2.2 ft)	
Gas Velocity - 1.4 m/s (4.5 ft/s)	
Solids Residence Time - 7 min	
Extent of Regeneration - 65%	
Total Regeneration System Fuel Burden - 95 Mg/d (105 T/d)	
(about 2.0% of the coal fed to the combustor)	
<u>Composition of Regenerator Flue Gas</u>	
8.0% SO ₂	
2.0% CO	
19.4% CO ₂	
8.8% H ₂ O	
61.8% N ₂	

^aThe fresh sorbent-feed mole ratio, hereinafter referred to as FR, is the mole fraction of CaO as fresh feed to the combustor, compared with the total CaO feed to the combustor including regenerated sorbent.

Table 2 shows the effects of changes in FR on regeneration system performance and dimensions. At low FR (e.g., 0.10), little fresh sorbent is needed and little sulfated sorbent is discarded. However, the lower the FR, the larger the regenerator since more sulfated sorbent is being circulated between the combustor and regenerator. In addition, regenerator fuel consumption will be higher because of the larger sorbent throughput, and the SO₂ concentration in the regenerator off-gas will be lower because (1) more inerts build up and (2) the sulfated sorbent releases less sulfur due to the lower reactivity of the stone.

Table 2. Predicted Effects of Feed Ratio on Regeneration System Performance and Dimensions

<u>Combustor</u>				<u>Regenerator</u>			
635 - MW AFBC				Bed Temperature - 1373 K			
Greer Limestone				Gas Inlet Temperature - 672 K			
Sewickley Coal				Solids Feed Temperature - 1116 K			
83% SO ₂ Retention				Solids Residence Time - 7 min			
Coal Feed Rate - 4779 Mg/d				Extent of Regeneration - 64.6%			
				Pressure - 103 kPa			
				Superficial Gas Velocity - 1.37 m/s			
FR	Fresh Sorbent Feed, Mg/d	Regenerator Feed, Mg/d	Waste, Mg/d	Regenerator Coal Usage, % of Combustor Usage	Regenerator Bed Area, m ²	Regenerator Bed Height, m	Regenerator Off-Gas SO ₂ Concentration, %
0.10	643	5249	703	3.48	45.7	0.76	7.08
0.20	907	3639	906	2.97	36.2	0.67	8.03
0.30	1171	2829	1121	2.50	29.6	0.63	8.38
0.40	1436	2245	1336	2.06	24.1	0.62	8.54
0.50	1700	1768	1549	1.66	19.2	0.61	8.60
0.60	1964	1352	1760	1.28	14.8	0.61	8.65
0.70	2228	977	1864	0.93	10.7	0.60	8.64
0.80	2492	632	2173	0.60	7.0	0.60	8.60
0.90	2756	307	2376	0.29	3.4	0.60	8.58

Conversely, at higher FR (e.g., 0.40), more fresh sorbent is needed and more sulfated sorbent is discarded. The regenerator would be smaller and the fuel consumption would decrease, while the off-gas SO_2 concentration would increase. Thus, at low FR, operating cost is low and capital cost is high, while at high FR, operating cost is high and capital cost is low. Therefore, the decision as to which FR to incorporate in the design must be made on the basis of economic factors. This type of analysis is made in a later section.

b. Predicted Effect of Superficial Gas Velocity on Regenerator Dimensions and Performance

The superficial gas velocity in a fluidized-bed regenerator can be varied between two limits. Previous work has shown that the bed tends to defluidize due to particle agglomeration at low gas velocities; at high gas velocities, there is excessive carryover loss due to particle entrainment. The range for superficial gas velocity is determined by coal-ash characteristics, as well as by spent sorbent particle size, reducing gas concentration, and bed temperature. Within the range allowed by these constraints, the effect of superficial gas velocity on regenerator configuration can be predicted.

Selection of a solids feed rate and solids residence time fixes the regenerator fluidized-bed volume. At a selected solids feed temperature, gas inlet temperature, and regenerator bed temperature, the gas residence time varies directly with solids residence time. It then follows that at a constant solids residence time, the gas residence time cannot vary if the off-gas SO_2 concentration is to remain the same. To utilize a higher gas velocity and maintain the same gas residence time, the bed would have to be made deeper and the bed cross-sectional area decreased since bed volume cannot change (constant solids feed rate and constant solids residence time). At constant gas and solids residence time, changes in the superficial gas velocity could only be accomplished by changing the dimensions of the regenerator if the same SO_2 concentration is to be maintained in the off-gas. For a low gas velocity, a regenerator would have a shallow bed and a large cross-sectional area; for a high gas velocity, a regenerator would have a deep bed and a small cross-sectional area. This is shown in Table 3. It should be kept in mind that good fluidization behavior still demands that a bed have a height to diameter ratio within a certain range.

A deep bed has a greater pressure drop across it than a shallow bed does. This would increase the operating cost and the capital cost for fans. Since the freeboard height is the main factor in determining the height of the bed enclosure, increased bed height would not entail a significant capital-cost penalty for the regenerator. Decreased bed cross-sectional area could significantly decrease capital cost. The superficial gas velocity would have to be finally determined on an economic basis within the constraints of avoiding defluidization, avoiding excessive particle carryover, and achieving good fluidization behavior.

Table 3. Predicted Effects of Superficial Gas Velocity on Regenerator Dimensions

<u>Combustor</u>		<u>Regenerator</u>	
635-MW AFBC		Bed Temperature - 1373 K	
Greer Limestone		Bed Pressure - 103 kPa	
Sewickley Coal		Gas Inlet Temperature - 672 K	
83% SO ₂ retention		Solids Feed Temperature - 1116 K	
FR - 0.20		Solids Residence Time - 7 min	
Coal Feed Rate - 4779 Mg/d		Superficial Gas Residence Time - 0.49 s	
		Extent of Regeneration - 64.6%	
		Solids Feed Rate - 3639 Mg/d	
		Coal Feed Rate - 142 Mg/d	
		Off-Gas SO ₂ Concentrations - 8.03%	

Superficial Gas Velocity, m/s	Expanded Bed Height, m	Regenerator Bed Area, m ²	Regenerator Bed Volume m ³
0.91	0.45	54.2	24.1
1.37	0.67	36.2	24.1
1.83	0.89	26.9	24.1
2.29	1.12	21.5	24.1
2.74	1.34	18.0	24.1

c. Predicted Effect of Solids Residence Time on Regenerator Dimensions and Performance

Previously reported data² obtained with the 10.8-cm-ID (4.25-in.) regenerator showed the effect of solids residence time on the SO₂ concentration in the regenerator off-gas. Sulfur dioxide concentration in the off-gas decreased with increased solids residence time. This result was obtained with a bed having a fixed diameter and height. To vary the solids residence time in the regenerator while operating at a fixed gas velocity, the solids feed rate as well as the inlet gas O₂ concentration had to be changed.

In the current analysis, the inlet gas is assumed to be air (21% O₂), the reactor configuration is allowed to vary, and the gas velocity is fixed at 1.37 m/s (4.5 ft/s). At an FR of 0.20 and with an air feed, the SO₂ concentration in the regenerator off-gas was found to increase with solids residence time, as shown in Table 4.

The effects of solids residence time on the requirements for expanded bed height, bed cross-sectional area, solids feed rate, and regenerator coal consumption (as a percentage of combustor coal consumption) are shown in Table 4. In general, increasing the solids residence time increases the required bed height substantially, changes the required bed cross-sectional area slightly, decreases the required solids feed rate, and increases the required regenerator coal usage. Increasing the solids residence time may also increase sorbent sintering, which might lead to decreased sorbent reactivity, but this has not been confirmed experimentally.

Table 4. Predicted Effects of Solids Residence Time on
Regenerator Dimensions and Performance

<u>Combustor</u>				<u>Regenerator</u>			
635-MW AFBC				Bed Temperature - 1373 K			
Greer Limestone				Superficial Gas Velocity - 1.37 m/s			
Sewickley Coal				Gas Inlet Temperature - 672 K			
83% SO ₂ Retention				Solids Feed Temperature - 1116 K			
FR - 0.20				Pressure - 103 kPa			
Coal Feed Rate - 4779 Mg/d							
Solids Residence Time, min	Superficial Gas Residence Time, s	Extent of Regeneration, %	Regenerator Solids Feed Rate, Mg/d	Regenerator Bed Height, m	Regenerator Bed Area, m ²	Regenerator Coal Usage, % of Combustor Coal Usage	Regenerator Off-Gas SO ₂ Concentration, mol %
3	0.24	37.5	4151	0.32	36.5	2.77	7.02
5	0.36	53.3	3803	0.50	36.3	2.90	7.69
7	0.49	64.6	3639	0.67	36.2	2.97	8.03
10	0.67	76.0	3515	0.92	36.1	3.02	8.30
15	0.98	86.3	3424	1.35	36.1	3.06	8.49
30	1.93	95.5	3359	2.65	36.0	3.10	8.64

d. Predicted Effects of Solids Feed Temperature and Gas Inlet Temperature on Regenerator Dimensions and Performance

The effects of changes in solids feed temperature and gas inlet temperature on requirements for regenerator bed height, bed cross-sectional area, and coal usage, as well as on SO_2 concentration in the off-gas, are shown in Table 5. In previous analyses, the solids feed temperature to the regenerator was assumed to be 1116 K (1550°F) (solids are fed directly to the regenerator from the combustor), and the gas inlet temperature was assumed to be 672 K (750°F). (The feed gas is preheated by sending it through a heat exchanger with the regenerator off-gas.) This results in a regenerator with a cross-sectional area of 36.2 m² (389 ft²), a bed height of 0.67 m (2.2 ft), an off-gas containing 8.0 mol % SO_2 , and a coal consumption 2.97% that of the combustor (7-min solids residence time, Table 4).

Table 5 shows that, if both the solids and the gas are fed into the regenerator at 294 K (70°F), the regenerator must have a cross-sectional area of 108.5 m² (1168 ft²) and a bed height of 0.22 m (0.72 ft). The coal consumption would increase to 9.07% that of the combustor, while the SO_2 concentration in the regenerator off-gas would decrease to 3.24 mol %. Conversely, if both the solids and gas are fed into the regenerator at its operating temperature of 1373 K (2012°F), the regenerator must have a cross-sectional area of 13.0 m² (140 ft²) and a bed height of 1.86 m (6.10 ft). The coal consumption would decrease to 1.04% that of the combustor, while the SO_2 concentration in the regenerator off-gas would increase to 16.85 mol %.

When the gas and solids are fed to the regenerator cold rather than hot, more coal must be fed to supply the sensible heat necessary to raise the temperature of the reactants. Similarly, additional air must be fed to react with this additional coal; this dilutes the off-gas and therefore reduces the SO_2 concentration in the off-gas. The total amount of SO_2 leaving the regenerator is the same for all cases shown in Table 5.

When gas and solids are fed to the regenerator hot, coal combustion must supply only the reducing gas plus the heat of reaction for the reductive decomposition. This decreases coal consumption. Less air is needed to react with this coal, and the SO_2 concentration in the off-gas increases because of less dilution.

The bed volumes are the same for all cases shown in Table 5, and solids feed rate and the residence time do not change. Since heating of the inlet gas and solids takes no appreciable time (heating is almost instantaneous for the gas and on the order of seconds for the solids), the effective gas and solids residence times for the reactions are not affected by the feed temperatures. Therefore, all cases shown in Table 5 are kinetically and thermodynamically equivalent with respect to reductive decomposition.

At the cold-feed condition in which a large amount of air is required to react with the extra coal, bed cross-sectional area must be increased to keep the gas velocity constant. Conversely, under the hot-feed conditions, considerably less air is required to react with the coal; bed cross-sectional area is much smaller, but bed height must be increased to maintain the regenerator volume constant. It should be noted that the

Table 5. Predicted Effects of Solids Feed Temperature and Gas Inlet Temperature on Regenerator Dimensions and Performance

<u>Combustor</u>			<u>Regenerator</u>		
635 - MW AFBC			Solids Residence Time - 7 min		
Greer Limestone			Regenerator Temperature - 1373 K		
Sewickley Coal			Superficial Gas Velocity - 1.37 m/s		
83% SO ₂ Retention			Solids Feed Rate - 3639 Mg/d		
FR - 0.20			Pressure - 103 kPa		
Coal Feed Rate - 4779 Mg/d					
Solids Feed Temperature, K	Gas Inlet Temperature, K	Regenerator Bed Height, m	Regenerator Bed Area, m ²	Regenerator Coal Usage, % of Combustor Usage	Regenerator Off-Gas SO ₂ Concentration, mol %
294	294	0.22	108.5	9.07	3.24
294	478	0.25	97.8	8.15	3.52
294	672	0.28	87.1	7.28	3.90
294	922	0.31	76.9	6.40	4.32
294	1373	0.39	62.4	5.19	5.15
589	294	0.28	87.1	7.25	3.90
589	478	0.31	78.4	6.51	4.25
589	672	0.34	70.1	5.83	4.67
589	922	0.39	61.9	5.12	5.18
589	1373	0.48	50.1	4.15	6.16
1116	294	0.54	44.8	3.69	6.76
1116	478	0.60	40.2	3.31	7.38
1116	672	0.67	36.2	2.97	8.03
1116	922	0.76	31.8	2.60	8.89
1116	1373	0.93	25.9	2.11	10.42
1373	294	1.07	22.6	1.83	11.51
1373	478	1.19	20.3	1.64	12.46
1373	672	1.32	18.3	1.47	13.44
1373	922	1.50	16.1	1.29	14.66
1373	1373	1.86	13.0	1.04	16.85

regenerator dimensions could be varied if changes of the gas velocity were allowed. Within previously mentioned constraints (including the constraint that all regenerator volumes be equal and not vary with gas velocity), increased gas velocity would require a deeper bed of smaller area, while decreased gas velocity would require a shallower bed of larger area.

From this analysis, it can be seen that the solids feed temperature and gas inlet temperature have a large effect on regenerator off-gas SO_2 concentration, regenerator coal consumption, and regenerator bed height and cross-sectional area. Solids feed temperature has a greater effect on the above variables than does gas inlet temperature since a greater amount of sensible heat is required to heat the solids to regenerator conditions than is required to heat the gas. It might be possible to preheat the feed gas to a higher temperature than 672 K (750°F) by passing it through tubes immersed in the combustor. Also, the solids might be preheated to more than 1116 K (1550°F) by passing them through a carbon burnup cell. It should be noted that this would result in no net change in coal consumption in the overall system (combustor-regenerator) since the sensible heat of the reactants would still have to be supplied. However, there would be an increase in SO_2 concentration in the regenerator off-gas that would result in lower gas flow rates in the regenerator and sulfur-recovery system. Since the cost of the sulfur-recovery system is the major capital equipment cost in the overall regeneration system, an increase in SO_2 concentration in the off-gas should result in a major cost savings.

e. Predicted Effect of Regenerator Bed Temperature on Regenerator Dimensions and Performance

The effects of regenerator bed temperature and solids residence time on extent of regeneration have been documented in a previous report.² At constant solids residence time, the extent of regeneration increases with higher bed temperatures; at a constant bed temperature, the extent of regeneration increases with longer residence times.

Table 6 illustrates the effect of bed temperature on regenerator dimensions and performance. The combustor operates at the same conditions for all cases. In the regenerator, the solids feed and gas inlet temperatures, superficial gas velocity, and solids feed rate do not change; the overall system FR is 0.20 for all cases; the extent of regeneration is made the same (64% for all cases) by increasing solids residence time to compensate for decreased operating temperature. In effect, changing the regenerator bed temperature has no effect on the combustor; only the regenerator is affected.

Solids residence time must be increased from 7 min at 1373 K (2012°F), to 10.7 min at 1348 K (1967°F), and to 17.2 min at 1323 K (1922°F) to keep the extent of regeneration constant at 64.6%. Because the solids feed rate is constant, regenerator bed volume must be increased to increase the solids residence time. Less coal would be burned to achieve the lower temperature; therefore, less air would be fed to combust the coal. To maintain the superficial gas velocity in the regenerator at 1.37 m/s (4.5 ft/s), the cross-sectional area of the bed would decrease from 36.2 m² (389 ft²) at 1373 K (2012°F), to 33.3 m² (358 ft²) at 1348 K (1967°F), and to 30.3 m² (326 ft²) at 1323 K (1922°F). However, since regenerator bed height would

Table 6. Predicted Effects of Regenerator Bed Temperature on Regenerator Dimensions and Performance

<u>Combustor</u>				<u>Regenerator</u>		
635-MW AFBC				Superficial Gas Velocity - 1.37 m/s		
Greer Limestone				Gas Inlet Temperature - 672 K		
Sewickley Coal				Solids Feed Temperature - 1116 K		
83% SO ₂ Retention				Solids Feed Rate - 3639 Mg/d		
FR - 0.20				Extent of Regeneration - 64.6%		
Coal Feed Rate - 4779 Mg/d				Pressure - 103 kPa		
Bed Temp, K	Solids Residence Time, min	Superficial Gas Residence Time, s	Regenerator Bed Height, m	Regenerator Bed Area, m ²	Regenerator Coal Usage, % of Combustor Usage	Regenerator Off-Gas SO ₂ Concentration, mol %
1373	7.0	0.49	0.67	36.2	2.97	8.03
1348	10.7	0.81	1.11	33.3	2.78	8.46
1323	17.2	1.42	1.95	30.3	2.60	8.96

increase from 0.67 m (2.2 ft) at 1373 K (2012°F), to 1.11 m (3.64 ft) at 1348 K (1967°F), and to 1.95 m (6.40 ft) at 1323 K (1922°F), superficial gas residence time must also be increased to provide the necessary time for reaction at the lower temperatures. Coal feed rate would decrease from 2.97% of that of the combustor at 1373 K (2012°F), to 2.78% at 1348 K (1967°F), and to 2.60% at 1323 K (1922°F). Because there would be less dilution at the lower bed temperatures, the SO₂ concentration in the off-gas would increase from 8.03% at 1373 K (2012°F), to 8.46% at 1348 K (1967°F), and to 8.96% at 1323 K (1922°F).

Regenerator performance would improve (i.e., there would be less coal consumption and a higher off-gas SO₂ concentration) at lower temperatures. Bed area would decrease somewhat, but bed height would increase substantially. This might result in a cost savings for the regenerator itself, but fan power would have to be increased. With a lower-temperature regenerator, the use of lower-cost construction materials and methods might be possible, sintering and agglomeration might decrease, and there might be less reactivity loss by the sorbent. Higher off-gas SO₂ concentrations would lower the cost of the sulfur-recovery system. It should be noted, however, that no experiments have been done at temperatures lower than 1323 K (1922°F). At temperatures below this, the concentration of SO₂ in the off-gas may be limited by thermodynamic equilibrium considerations.

f. Predicted Effect of Pressure on Regenerator Dimensions and Performance

At low pressures (lower than 206 kPa or approximately 2 atm), the effect of increasing the pressure in the regenerator is the same as the effect of increasing the superficial gas velocity. That is, a change in design pressure has no effect on regenerator performance. An increase in pressure calls for a deeper regenerator bed with a smaller cross-sectional area; the bed volume remains the same. A decrease in pressure would call for a shallower but larger-bed cross section. This is illustrated in Table 7. These results cannot be extrapolated to high pressures since thermodynamic equilibrium would limit the concentration of SO₂ obtainable.

Table 7. Predicted Effect of Pressure on Regenerator Dimensions

<u>Combustor</u>		<u>Regenerator</u>		
635-MW AFBC		Bed Temperature - 1373 K		
Greer Limestone		Gas Inlet Temperature - 672 K		
Sewickley Coal		Solids Feed Temperature - 1116 K		
FR - 0.20		Superficial Gas Velocity - 1.37 m/s		
Coal Feed Rate - 4779 Mg/d		Solids Residence Time - 7 min		
		Extent of Regeneration - 64.6%		
		Solids Feed Rate - 3639 Mg/d		
		Coal Feed Rate - 142 Mg/d		
		Off-Gas SO ₂ Concentration - 8.03%		

Condition	Pressure, kPa	Regenerator Bed Area, m ²	Regenerator Bed Height, m	Regenerator Bed Volume, m ³
1a	52	72.7	0.33	24.1
1b	103	36.2	0.67	24.1
1c	155	24.0	1.01	24.1
1d	206	18.0	1.34	24.1

g. Predicted Effect of Changes in Feed-Gas Oxygen Concentration on Regenerator Dimensions and Performance

In general, air would be the feed gas to a large-scale regenerator. However, changes in feed-gas oxygen concentration were evaluated as to their effect on regenerator dimensions and performance as a preliminary step in a possible economic study of using oxygen-enriched feed gas in a regenerator. As can be seen in Table 8, oxygen enrichment of the feed gas results in an increase in off-gas SO₂ concentration and a decrease in coal consumption. Coal consumption would decrease because less sensible heat would be needed to preheat the inert nitrogen. Off-gas SO₂ concentration would increase because of less dilution by nitrogen. Bed cross-sectional area would decrease (at constant superficial gas velocity) because less inert nitrogen would pass through the bed. Bed height would increase to maintain a constant bed volume (constant solids residence time) and provide the longer gas residence time necessary to obtain high off-gas SO₂ concentrations.

Oxygen enrichment of the feed gas could increase the off-gas SO₂ concentration considerably. This would bring about a great cost savings in the sulfur-recovery system (RESOX or other), which is the major capital cost item in a regeneration system. Therefore, an overall economic evaluation should be made of using oxygen-enriched feed gas for the regenerator.

Table 8. Predicted Effect of Changes in Feed-Gas Oxygen Concentration on Regenerator Dimensions and Performance

<u>Combustor</u>			<u>Regenerator</u>		
635-MW AFBC			Bed Temperature - 1373 K		
Greer Limestone			Gas Inlet Temperature - 672 K		
Sewickley Coal			Solids Feed Temperature - 1116 K		
FR - 0.20			Solids Residence Time - 7 min		
Coal Feed Rate - 4779 Mg/d			Extent of Regeneration - 64.6%		
			Solids Feed Rate - 3639 Mg/d		
			Pressure - 103 kPa		
			Superficial Gas Velocity - 1.37 m/s		
Inlet Gas O ₂ Concentration, %	Superficial Gas Residence Time, s	Regenerator Bed Area, m ²	Regenerator Bed Height, m	Regenerator Off-Gas SO ₂ Concentration mol %	Regenerator Coal Usage, % of Combustor Usage
15.1	0.29	60.9	0.40	5.22	3.66
21.0	0.49	36.2	0.67	8.03	2.97
40.0	1.12	15.8	1.53	14.66	2.40
60.3	1.79	9.8	2.45	19.33	2.23
80.1	2.44	7.2	3.35	22.53	2.16
99.2	3.08	5.7	4.22	24.86	2.12

3. Predicted Effects of Off-Design Conditions on Regenerator Operating Parameters

In this section, the effects of changes in operating variables on performance of an operating reactor with fixed bed height and cross-sectional area are discussed. The effects of changing the solids feed rate, solids feed temperature, gas inlet temperature, and regenerator bed temperature will be explored for a regenerator which could be designed to operate with a 635-MW AFBC using Greer limestone and Sewickley coal at an FR of 0.20. For the baseline conditions (case Ia, Table 9) of an operating temperature of 1373 K (2012°F), a solids feed temperature of 1116 K (1550°F), a gas inlet temperature of 672 K (750°F), a solids residence time of 7 min, a solids feed rate of 3639 Mg/d, and a superficial gas velocity of 1.37 m/s (4.5 ft/s), the regenerator will (1) have a bed height of 0.67 m (2.2 ft) and an area of 36.2 m² (389 ft²), (2) require 142 Mg/d of coal, and (3) have an off-gas SO₂ concentration of 8.03%.

a. Predicted Effects of a Lower Solids Feed Rate on Regenerator Operating Parameters

Cases Ia, Ib, Ic, Id, and Ie in Table 9 illustrate the effects on regenerator operating parameters of turning the combustor down (reducing the electrical and/or steam production of the system). Reducing the load on the combustor would reduce the solids feed rate to the regenerator. Since the regenerator volume would be constant (the volume cannot be altered during operation), the solids residence time would increase, which would mean a concomitant increase in gas residence time. Since bed height would remain constant, superficial gas velocity must be lowered. Coal feed rate would decrease, while off-gas SO₂ concentration would increase.

Decreasing the combustor output by 50% would decrease the solids feed rate to the regenerator from 3639 Mg/d to 1713 Mg/d; simultaneously, the coal feed rate to the regenerator would be reduced from 142 Mg/d to 73 Mg/d and the SO₂ concentration in the off-gas would increase from 8.03 to 8.48%. The superficial gas velocity would decrease from 1.37 m/s (4.5 ft/s) to 0.68 m/s (2.23 ft/s). This lower velocity might result in defluidization. The amount a system can be turned down will be determined by the relation of operating velocity to defluidization velocity.

Table 9. Predicted Effects of Off-Design Conditions (Solids Feed Rate, Gas Inlet Temperature, Solids Feed Temperature, and Regenerator Bed Temperature) on Regenerator Performance

Combustor							Regenerator				
635-MW AFBC Greer Limestone Sewickley Coal FR - 0.20 Coal Feed Rate - 4779 Mg/d							Bed Height - 0.67 m Bed Area - 36.2 m ² Pressure - 103 kPa				
Condition	Combustor Output, %	Solids Residence Time, min	Superficial Gas Residence Time, s	Regenerator Bed Temp., K	Solids Feed Temp., K	Gas Inlet Temp., K	Regenerator Solids Feed Rate, Mg/d	Superficial Gas Velocity, m/s	Regenerator Coal Usage, % of Combustor Usage	Regenerator Coal Feed, Mg/d	Regenerator Off-Gas SO ₂ Conc., mol %
Ia	100	7.0	0.49	1373	1116	672	3639	1.37	2.97	142	8.03
Ib	90	7.9	0.54	1373	1116	672	3233	1.23	2.99	129	8.14
Ic	75	9.6	0.65	1373	1116	672	2644	1.03	3.01	108	8.28
Id	50	14.9	0.98	1373	1116	672	1713	0.68	3.06	73	8.48
Ie	33	22.6	1.47	1373	1116	672	1125	0.45	3.09	49	8.60
IIa	100	7.0	0.96	1373	1373	672	3639	0.69	1.47	70	13.44
IIb	100	7.0	0.49	1373	1116	672	3639	1.37	2.97	142	8.03
IIc	100	7.0	0.25	1373	589	672	3639	2.68	5.83	279	4.67
IIIa	100	7.0	0.68	1373	1116	1373	3639	0.98	2.11	101	10.42
IIIb	100	7.0	0.55	1373	1116	922	3639	1.21	2.60	124	8.89
IIIc	100	7.0	0.49	1373	1116	672	3639	1.37	2.97	142	8.03
IIId	100	7.0	1.44	1373	1116	478	3639	1.53	3.31	158	7.38
IVa	100	7.0	0.16	1373	294	294	3639	4.17	9.07	433	3.24
IVb	100	7.0	1.36	1373	1373	1373	3639	0.49	1.04	50	16.70
Va	65	10.7	0.81	1348	1116	672	2374	0.82	2.78	87	8.46
Vb	41	17.2	1.42	1323	1116	672	1485	0.47	2.60	51	8.96

b. Predicted Effects of Solids Feed Temperature on Regenerator Operating Parameters

Cases IIa, IIb, and IIc in Table 9 illustrate the effects of solids feed temperature on regenerator operating parameters. Case IIb is the standard condition for which the regenerator was designed. Increasing the solids feed temperature from 1116 K (1550°F) to 1373 K (2012°F), (Case IIa), at a gas feed temperature of 672 K (750°F) would reduce the amount of sensible heat that must be provided by coal combustion, thereby reducing the regenerator coal feed rate from 142 Mg/d to 70 Mg/d. Less air would be needed to combust this quantity of coal; since the bed cross-sectional area would be constant, the superficial gas velocity would be decreased from 1.37 m/s (4.5 ft/s) to 0.69 m/s (2.26 ft/s). Because there would be less dilution, the off-gas SO₂ concentration would increase from 8.03 to 13.44%.

Decreasing the solids feed temperature from 1116 K (1550°F) to 589 K (600°F) (case IIc) would increase the amount of sensible heat that must be provided by coal combustion, thereby increasing the regenerator coal feed rate from 142 Mg/d to 279 Mg/d. More air would be needed to combust this coal; since the bed cross-sectional area would be constant, the superficial gas velocity would increase from 1.37 m/s (4.5 ft/s) to 2.68 m/s (8.79 ft/s). Because there would be more dilution, the off-gas SO₂ concentration would decrease from 8.03 to 4.67%.

c. Predicted Effects of Gas Inlet Temperature on Regenerator Operating Parameters

The effects of gas inlet temperature on regenerator operating parameters are similar, albeit smaller than those of solids feed temperature. Higher gas inlet temperature would reduce coal consumption, reduce superficial gas velocity, and increase off-gas SO₂ concentration. This is illustrated by cases IIIa, IIIb, IIIc, and IIId in Table 9.

Cases IVa and IVb in Table 9 illustrate the effects of extreme feed conditions on regenerator operating parameters. Feeding both gas and solids at 294 K (70°F) would increase the coal consumption to 433 Mg/d and the superficial gas velocity to 4.17 m/s (13.7 ft/s), and would reduce the off-gas SO₂ concentration to 3.24%; feeding both the gas and the solids at 1373 K (2012°F) would decrease coal consumption to 50 Mg/d and the superficial gas velocity to 0.49 m/s (1.61 ft/s) and would increase the SO₂ concentration in the off-gas to 16.70%.

d. Predicted Effects of Regenerator Bed Temperature on Regenerator Operating Parameters

Cases Va and Vb in Table 9 illustrate the effects of regenerator bed temperature on regenerator operating parameters. A previous section demonstrated how the design of a regenerator should be changed to operate at various temperatures (Table 6). In this section, it is assumed that a regenerator designed to operate at 1373 K (2012°F) will be operated at 1348 K (1967°F) and 1323 K (1922°F); the attendant changes in operating parameters will be assessed.

Case Ia in Table 9 is considered to be the baseline condition. Steam and/or electrical production in the plant would be decreased to 65% of the baseline condition for operation at 1348 K (1967°F) and to 41% of baseline for operation at 1323 K (2012°F). Regenerator coal consumption would decrease from 142 Mg/d at 1373 K (2012°F) to 87 Mg/d at 1348 K (1967°F) and to 51 Mg/d at 1323 K (1922°F). Sulfur dioxide concentration in the off-gas would increase from 8.03% at 1373 K (2012°F) to 8.46% at 1348 K (1967°F) and to 8.96% at 1323 K (1922°F), while gas velocity would decrease from 1.37 m/s (4.5 ft/s) at 1373 K to 0.82 m/s (2.69 ft/s) at 1348 K (1967°F) and to 0.47 m/s (1.54 ft/s) at 1323 K (1922°F).

e. Design of a Regenerator to Accommodate Turndown

For operation of a regenerator at reduced load (lower solids feed rate), the superficial gas velocity must be decreased. However, the gas velocity must always remain above the defluidization velocity (below the defluidization velocity, the bed material does not fluidize but agglomerates); this limits the turndown that a system can tolerate. In Table 10, the minimum gas velocity is assumed to be 1.37 m/s (4.5 ft/s). Case I in Table 10 provides for a maximum of 25% turndown--i.e., the system will reach minimum gas velocity at a system load of 75%. Case II provides for 50% turndown, while case III provides for 67% turndown. This is accomplished by adjusting the bed configuration to accommodate a higher superficial gas velocity under full-load conditions. For no turndown capability (see case Ib in Table 7), the bed height is 0.67 m (2.2 ft), the bed cross-sectional area is 36.2 m² (389 ft²), and the superficial gas velocity is 1.37 m/s (4.5 ft/s). The bed height would be increased from 0.67 m (2.2 ft) to 0.89 m (2.92 ft) to accommodate 25% turndown, to 1.34 m (4.40 ft) for 50% turndown, and to 2.02 m (6.65 ft) for 67% turndown. The bed cross-sectional area would decrease from 36.2 m² (389 ft²) to 27.1 m² (292 ft²) to accommodate 25% turndown, would decrease to 17.9 m² (193 ft²) for 50% turndown, and to 12.0 m² (129 ft²) for 67% turndown. The full-load superficial gas velocity would increase from 1.37 m/s (4.5 ft/s) to 1.82 m/s (5.97 ft/s) to accommodate 25% turndown, to 2.73 m/s (8.96 ft/s) for 50% turndown, and to 4.12 m/s (13.5 ft/s) for 67% turndown. The solids feed rate, the solids residence time, the gas residence time, the bed volume, the coal consumption, and the SO₂ concentration in the off-gas are the same for the full-load part of each case (Ia, IIa, IIIa). Excessive particulate carryover as a result of too high a superficial gas velocity and excessive pressure drop from too deep a bed are the practical limitations on regenerator turndown capability.

Table 10. Design of Regenerator to Accommodate Turndown

Combustor				Regenerator							
635-MW AFBC				Bed Temperature - 1373 K							
Greer Limestone				Gas Inlet Temperature - 672 K							
Sewickley Coal				Solids Feed Temperature - 1116 K							
FR - 0.20				Minimum Superficial Gas Velocity - 1.37 m/s							
Coal Feed Rate - 4779 Mg/d				Pressure - 103 kPa							

Condition	Combustor Output %	Solids Residence Time, min	Superficial Gas Residence Time, s	Regenerator Solids Feed Rate, Mg/d	Regenerator Bed Height, m	Regenerator Bed Area, m ²	Superficial Gas Velocity, m/s	Regenerator Coal Feed Rate, Mg/d	Regenerator Coal Usage, % of Combustor Usage	Regenerator Off-Gas SO ₂ , mol %	Turndown Desired
Ia	100	7.0	0.49	3639	0.89	27.1	1.82	142	2.97	8.03	25%
Ib	90	7.9	0.54	3233	0.89	27.1	1.65	129	2.99	8.14	
Ic	75	9.6	0.65	2644	0.89	27.1	1.37	108	3.01	8.28	
IIa	100	7.0	0.49	3639	1.34	17.9	2.73	142	2.97	8.03	50%
IIb	90	7.9	0.54	3233	1.34	17.9	2.48	129	2.99	8.14	
IIc	75	9.6	0.65	2644	1.34	17.9	2.06	108	3.01	8.28	
IId	50	14.9	0.98	1713	1.34	17.9	1.37	73	3.06	8.48	
IIIa	100	7.0	0.49	3639	2.02	12.0	4.12	142	2.97	8.03	67%
IIIb	90	7.9	0.54	3233	2.02	12.0	3.74	129	2.99	8.14	
IIIc	75	9.6	0.65	2644	2.02	12.0	3.11	108	3.01	8.28	
IIId	50	14.9	0.98	1713	2.02	12.0	2.06	73	3.06	8.48	
IIIe	33	22.6	1.47	1125	2.02	12.0	1.37	49	3.09	8.60	

4. Comparison of New and Earlier Predictions of Effects of Process Parameters

Predictions presented earlier in this report (Sections 2 and 3) differ in certain instances from predictions made in previous reports. This section explores the new predictions, compares them with previous predictions in certain instances and explains the differences.

Since the volume of the regenerator used in these studies is fixed (constant bed area and expanded bed height), the minimum number of variables that can be simultaneously studied is two. For instance, the effect of solids residence time may be studied only if (1) superficial gas velocity, (2) regenerator bed temperature, or (3) feed-gas oxygen concentration is also varied. The solids residence time in a fixed-volume reactor can only be increased by decreasing the solids feed rate; this simultaneously lowers the sensible heat requirement, and a lower coal feed rate and less combustion air are needed. Combustion air can be decreased in two ways: by lowering gas velocity or by lowering oxygen concentration in the feed gas. Since lowering of gas velocity might alter fluidization characteristics or cause agglomeration of material by defluidization, feed-gas oxygen concentration was chosen as the operating variable.

For conditions which call for increasing the amount of combustion air, doing so by increasing the gas velocity might lead to excessive particle carryover; instead, oxygen concentration in the feed gas can be varied.

Changing the regenerator bed temperature (the second variable) would affect gas-solid kinetics and would not be a reasonable approach to establishing the effect of solids residence time on the extent of regeneration and off-gas SO_2 concentration.

A model has been developed from the PDU experimental results and has been used to predict the results of other experiments; agreement has been good.¹ In all experimental work, the feed gas oxygen concentration has been varied. This a useful experimental tool, but for the design of larger systems, the feed gas should be air, fixing the feed-gas oxygen concentration at 21%. Results reported previously,² as well as results presented earlier in this report (Sections 2 and 3), all assume that the feed gas is air.

a. Relation of Solids Residence Time and Gas Residence Time to Regenerator Performance

The relationship of solids residence time to superficial gas residence time at a regenerator temperature of 1373 K (2012°F), a solids feed temperature of 1116 K (1550°F), and a gas inlet temperature of 672 K (750°F) for a conceptual 635-MW regenerator may be seen in Table 4. Analogous tables could be made for different regenerator temperatures and different solids feed and gas inlet temperatures. Also, relationships between solids residence time, regenerator temperature, and extent of regeneration have been previously reported.¹ In comparing regenerator performance, it should be kept in mind that two regenerators that are operated at the same temperature, with the same solids feed and gas inlet temperatures, and with the same gas and solids residence time are kinetically equivalent. That is, the extent of regeneration, SO_2 concentration in the off-gas, and coal/solids feed ratio

will be identical. Larger regenerators, such as that assumed in Table 4, would have slightly lower heat losses and therefore would be more efficient (have higher off-gas SO_2 concentrations), but this effect would be small in practical-size units.

b. Relation of Bed Height to Superficial Gas Velocity

This brings us to the relationship of bed height to superficial gas velocity. Once a gas residence time has been fixed, expanded bed height is directly proportional to superficial gas velocity. This is shown in Table 3 for a conceptual 635-MW combustor. Since the mass flow rate of gas remains constant, bed cross-sectional area decreases. The solids residence time is not changed thereby since the volume of the bed remains constant. Earlier work² in which bed height was increased ran into two problems: (1) only the height of the reducing zone was increased; the height of the oxidizing zone remained constant, and (2) increasing the height of a very-small-cross-sectional-area bed decreased the quality of fluidization (already poor) still further. The first problem has not been solved; it is hoped that the reducing and oxidizing zones can be made the appropriate sizes by adjusting the reducing gas concentration in the off-gas. The second problem should be solved by building larger regenerators for which the bed height/diameter ratios are not in the "slugging" regime.

Superficial gas velocity must be maintained between the lower velocity limit set by defluidization (which results in agglomeration) and the upper velocity limit set by particle carryover. In previous studies,² increases in gas velocity were found to be detrimental to performance. This was probably due to degradation of already-poor fluidization characteristics of the experimental PDU. Also, an increase in superficial gas velocity not accompanied by an increase in bed height decreases gas residence time; this, in turn, adversely affects bed performance.

c. Relation of Solids Residence Time to Off-Gas SO_2 Concentration

Sulfur dioxide concentration in the regenerator off-gas is predicted to increase with longer solids residence time (Table 4). In contrast, a previous report² implies that shorter solids residence times produce higher off-gas SO_2 concentrations. In earlier work, the experimental solids residence time was decreased by increasing the solids feed rate (at a fixed regenerator volume). This increased the amount of coal that had to be burned to provide sensible heat to the solids. Also, the oxygen concentration in the feed gas was increased so that the superficial gas velocity would not have to be increased. Since less nitrogen was present to dilute the off-gas, a higher SO_2 concentration resulted. If the SO_2 concentration obtained in the earlier work should be corrected to a 21% oxygen-feed-gas basis and the regenerator configuration should be "readjusted" to provide the correct gas residence time, SO_2 concentration in the off-gas would increase with longer solids residence times.

d. Relation of Solids Feed Temperature and Gas Feed Temperature to Off-Gas SO₂ Concentration

Sulfur dioxide concentration in the regenerator off-gas has been predicted to increase with solids feed temperature and gas inlet temperatures (Table 5). In comparison, previous work¹ implies that this effect is marginally important. If the solids residence time is fixed, the amount of sensible heat which must be supplied is inversely proportional to the solids feed temperature and gas feed temperatures. When more sensible heat was required in the experimental PDU, more coal was fed and a higher concentration of oxygen was used in the feed gas (the superficial gas velocity was constant). Therefore, the (cold-feed) runs which required the most preheat were diluted the least. Conversely, the runs which required the least preheat (hot-feed) suffered the most dilution. These effects tended to cancel each other, and at all feed conditions, SO₂ concentrations in the off-gas were similar.² If air is the only feed gas permitted and the regenerator configuration is adjusted appropriately, SO₂ concentration in the off-gas would increase with solids feed temperature and gas inlet temperature, as shown in Table 5.

e. Relation of Regenerator Bed Temperature to Off-Gas SO₂ Concentration

Previous work² predicted that off-gas SO₂ concentration would decrease with lower regenerator bed temperature. The extent of regeneration increases with longer residence times at all temperatures of interest. However, if there is a constant solids feed rate in the regenerator irrespective of temperature and if the regenerated product has to be returned to the combustor at the same composition, lower-temperature regeneration would result in a higher off-gas SO₂ concentration. A longer solids residence time must be utilized at lower regeneration temperatures in order to keep the same solids feed rate, composition, reactivity, and extent of regeneration. Since a lower regeneration temperature requires that less sensible heat be added, less coal and therefore less air must be fed to the regenerator. Less dilution of the off-gas results in higher SO₂ concentrations in the off-gas. This is illustrated in Table 6. However, bed volume would increase (to obtain a longer solids residence time); the bed would be deeper and somewhat smaller in cross-sectional area.

In a system which utilized the same solids residence time at the temperatures being compared, lower SO₂ concentrations would be obtained in the off-gas at lower regeneration temperatures. In addition, higher solids circulation rates would have to be maintained between the combustor and the regenerator at the lower regenerator temperature. At the lower temperature, regenerator cross-sectional area would have to decrease and regenerator bed height increase.

f. Conclusion

In conclusion, the PDU experimental data are valid and are useful for design purposes if all conditions are corrected to correspond to a feed gas containing 21% oxygen. The data relating solids residence time, gas residence time, solids feed temperature, gas inlet temperature, regenerator temperature, and superficial gas velocity to regenerator dimensions and performance can be utilized to design regenerators within operating and economic constraints.

5. Economic Feasibility of Regenerating Sulfated Limestone

An economic evaluation of regeneration of spent sorbent from fluidized-bed combustion was performed,⁴ using a Westinghouse cost study along with data from ANL cyclic combustion and regeneration experiments with Greer limestone and Sewickley coal. The system assumed was an atmospheric-pressure, fluidized-bed reductive-decomposition process, followed by a RESOX sulfur-recovery system with tail-gas incineration.

Capital cost for the system, capacity factor, and sorbent price (including sorbent disposal cost) were found to be important factors; fuel price and sulfur credit value were found to be of lesser importance. At today's capital cost, a 70% plant capacity factor, \$27.56/Mg coal price, and with no sulfur credit, the sorbent regeneration system would break even at a total sorbent cost of \$12.68/Mg. Further results were presented for values of all of the above parameters.

A computer program was developed to incorporate cyclic combustion and regeneration experimental data for a given coal and a given sorbent in order to predict the economic viability of regeneration with that particular coal and sorbent. A second computer program was written to predict the costs of a regeneration system when system size, various economic factors, coal type, sorbent type, and preliminary data (or assumptions) on sorbent reactivity are given. More detailed results have been previously reported.

TASK B. ALTERNATIVE REGENERATION PROCESS DEVELOPMENT
(D. S. Moulton)

1. Rotary-Kiln Regeneration

Previous emission-control studies have shown that spent limestone sorbents can be regenerated, using reducing agents. Rotary kilns are being evaluated for use as regeneration reactors. They can be externally fired, allowing reaction heat to be supplied without diluting the off-gas with combustion products. An externally fired rotary kiln has a potential for producing SO_2 in a concentrated stream. The ease of handling elemental sulfur, and the utilities' traditional avoidance of chemical processing, makes elemental sulfur an attractive final form of the sulfur pollutants. Concentrating the SO_2 stream simplifies the subsequent reduction to elemental sulfur and greatly improves the economics.

Studies are being conducted with a small laboratory-scale rotary kiln in support of further work with a larger industrial kiln. These studies are (1) to demonstrate rotary-kiln regeneration on a laboratory scale and (2) to provide information on kiln performance under various operating conditions. The SO_2 concentration in the off-gas is measured, and the extent of regeneration is determined by sulfur analysis of the solid product.

a. Equipment

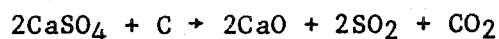
The laboratory-scale rotary kiln was constructed from a 26-mm-ID tube of fused silica. Heat was supplied by a 40-cm annular furnace, and the tube was rotated by a variable-speed motor via gear reductions and a pulley. The rotation rate was variable--between about 4 and 80 rpm. The kiln was fitted with rotary seals at each end. Solids feed rate was controlled by a rotating bucket driven by a variable-speed motor. The nitrogen carrier gas could be introduced at either end of the kiln and made to flow either concurrently or countercurrently to the solids flow. Countercurrent flow operation has been difficult to achieve, and most of the data has been obtained using cocurrent flow.

A 7-mm quartz gas-sampling tube was used to withdraw part of the off-gas from different points within the kiln. The tube extended into the kiln from the end, just above the solid reactants. The SO_2 content was measured with a Thermo Electron Corporation Model 40 pulsed fluorescence analyzer. Off-gas for analysis was drawn into the tube and was diluted with house nitrogen to bring the percent SO_2 within the range of the analyzer.

b. Materials and Procedure

Greer limestone, which had been sulfated in a fluidized-bed combustor, was supplied by Pope, Evans, and Robbins. The reductant was char from Occidental Research Corporation's flash-pyrolysis process. An SO_2/N_2 mixture used for analyzer calibration was obtained from Matheson and certified as 3.02% SO_2 .

The sulfated stone was analyzed for sulfate content by titration with a solution of barium perchlorate in isopropanol, using thorin and methylene blue as indicator. The stone was mixed with the char before it was added to the feeder. The mixing ratio was based on the sulfate analysis of the stone and the fixed carbon content of the char and was stoichiometric for the reaction:



except where noted otherwise. After passing through the kiln, samples of the solid product were analyzed for sulfate content by the above method. Some sulfide is formed by the following reaction:



The sulfide content was obtained from the difference between the sulfate content before and after oxidation at 850°C.

Preliminary work indicated that low rotation rates and small inclination angles were required to produce a solids residence time sufficient for regeneration. The kiln was generally operated at 4-10 rpm and at an inclination angle of 0.5 to 2.0 deg.

c. Kiln Operation

The laboratory-scale kiln was operated at room temperature to measure solids residence time under various operating conditions. Whatley⁵ has shown that the ratio of the dimensionless velocity number to the slope is nearly constant over a wide operating range:

$$\frac{V_v}{\tan \alpha} = \text{const} = C_v$$

where α is the kiln's angle of inclination measured from the horizontal, C_v is here referred to as the velocity ratio, and V_v is the velocity number given by:

$$V_v = \frac{v}{\omega D}$$

The solids velocity, v , is the kiln length, L , divided by the residence time, ω is the kiln rotation rate, and D the inside diameter.

Room temperature studies were made to investigate the above relationships. Residence time was determined from the mass flow rate and the total amount of material in the kiln. C_v measurements were made at various angles of inclination and the results, shown in Fig. 2, indicate that C_v is independent of the angle of inclination only when the angle exceeds about three degrees.

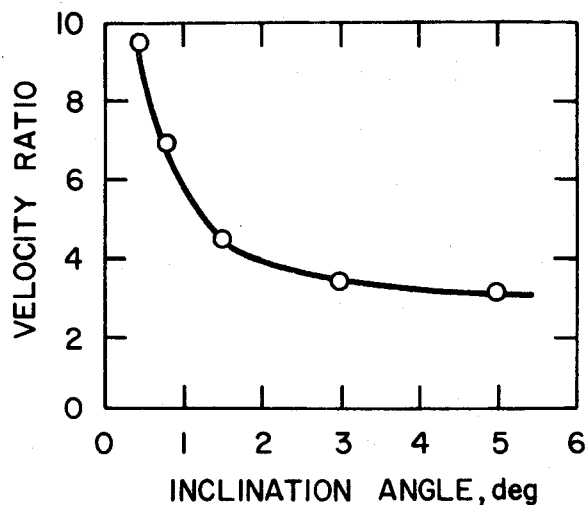


Fig. 2. Velocity Ratio vs. Inclination Angle in a Laboratory-Scale Rotary Kiln

The residence time, t , is given by

$$t = \frac{L}{\omega DC_v \tan \alpha}$$

For inclination angles greater than three degrees, C_v can be taken as 3.1; otherwise, C_v is obtained from Fig. 2. Griswold⁶ gives a similar equation which includes the angle of repose of the dry material. Whatley's treatment was used here because it is based on a dimensionless analysis and may be more useful for scale-up. Figure 2 was obtained for sulfated limestone having a 45° angle of repose, and C_v values obtained from the graph may have to be adjusted for material having significantly different angles of repose.

d. Results and Discussion

Four runs were made with the SO₂ sampling tube within the hot zone. The carrier-gas flow was adjusted to obtain the maximum percent SO₂, and was usually about 0.2 L/min. The results (Table 11) show that high SO₂ concentrations occur within the kiln. Gas grab samples taken just downstream from the kiln for mass spectrometric analysis were in general agreement with SO₂ levels indicated by the pulsed fluorescence analyzer. Data from the last three runs (Table 11) indicate that SO₂ concentrations near the equilibrium value of about 20%⁷ can be achieved within the kiln.

Table 11. Regeneration of Sulfated Greer Limestone with Char in a Small Rotary Kiln

Run	Temperature, °C	Operating Time, min	Residence Time, min	Regeneration, %	SO ₂ Concentration, in Off-Gas %
780414	1035	60	19	42	11 ^{a,b}
780418	1040	40	33	20	20 ^b
780419	1040	120	60	37	22 ^b 19 ^c
780425	1040	180	16	23	29 ^b

^aSulfur dioxide reacted with the stainless steel sampling tube. Quartz sampling tubes were used in subsequent runs.

^bMeasured with pulsed fluorescence analyzer.

^cMeasured with mass spectrometer.

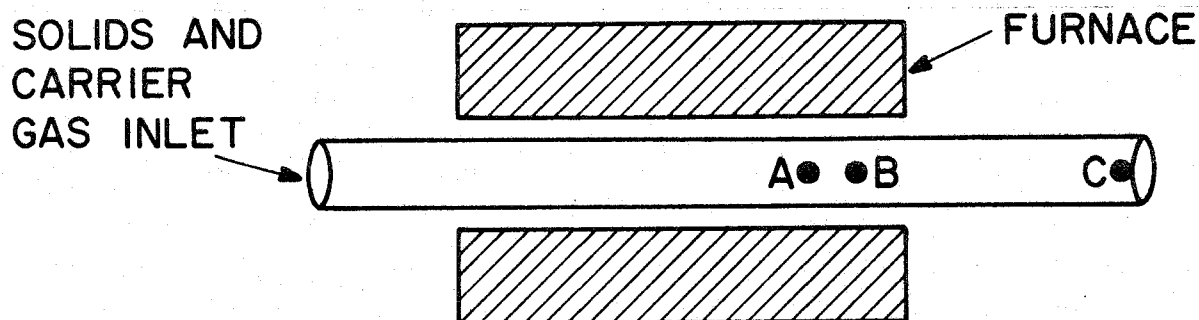


Fig. 3. Gas-Sampling Locations and Reactor Temperatures in the Laboratory-Scale Rotary Kiln Operated at 1040°C and 4 rpm.

A - 10 cm from end of heated zone, 1040°C

B - 5 cm from end of heated zone, 1005°C

C - Outlet, room temperature

In rotary kilns, it is difficult to separate the gas from the solid at high temperature. Ordinarily, the product gases circulate over some solid materials which are cooler than the reaction temperature before leaving the kiln. This could lead to recombination of the SO_2 with the cooler material, and experiments were made to see if this was a significant limitation.

The kiln was operated at 4 rpm and 1040°C with a solids residence time of about 20 min. Three different gas-sampling points, shown in Fig. 3, were used in different runs. The carrier-gas flow rate was varied during each run, to obtain a plot of percent SO_2 versus flow rate at each sampling point.

The results are shown in Fig. 4. At low carrier-gas flow rates, the SO_2 concentration inside the kiln approached 20%, approximately the equilibrium value. However, by the time the gas reached the kiln outlet, most of the SO_2 had recombined with the solid. At higher flow rates, there

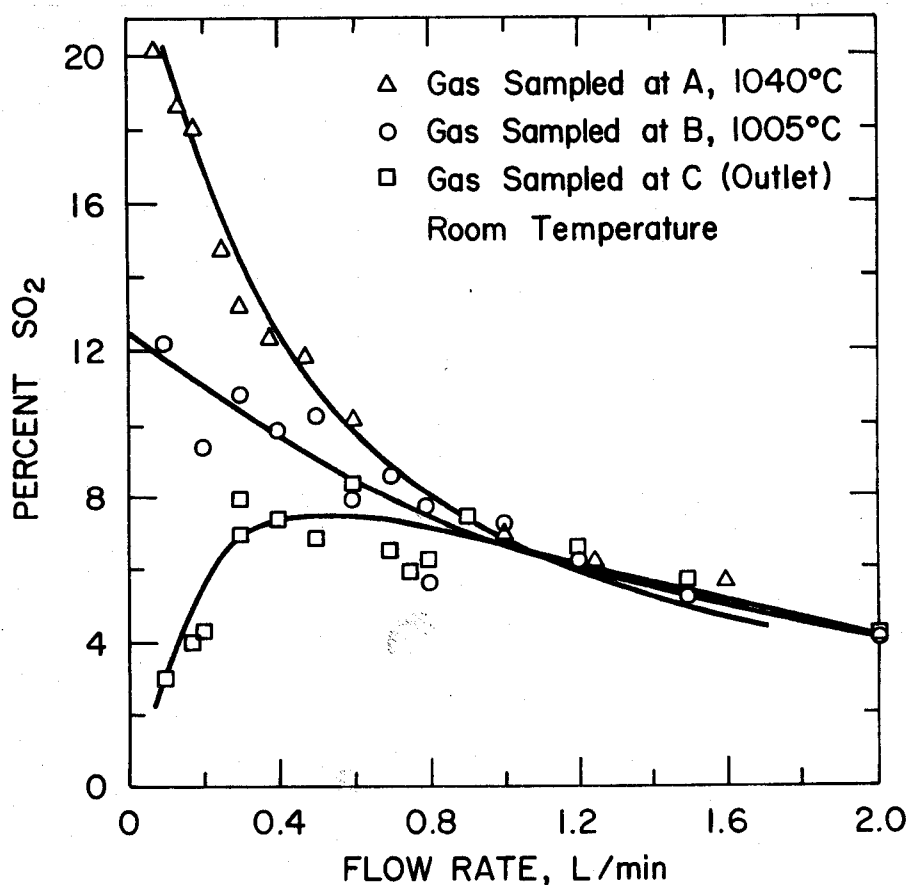


Fig. 4. Variation of Percent SO_2 in Off-Gas with Carrier-Gas Flow Rate, during Limestone Regeneration in a Small Rotary Kiln at 1040°C . Sampling locations are shown in Fig. 4.

was not sufficient time for the gas in the kiln to reach a high SO_2 concentration; however, there was also less SO_2 recombination during exit. In the laboratory-scale kiln, recombination with the solid was insignificant only at the higher carrier gas flow rates where the SO_2 concentration reached less than one-half the equilibrium value.

The amount of recombination in a larger kiln may differ from the above results. An increased gas residence time should allow high internal SO_2 concentrations at higher gas flow rates. If the solids are heated rapidly so that the lower-temperature material occupies only a short section of the kiln or if the incoming solids are saturated with SO_2 , the SO_2 stream might exit from the reactor without much recombination occurring. Otherwise, recombination may limit the maximum SO_2 concentration in the off-gas.

High rates of regeneration occur with low percentages of SO_2 in the off-gas, when the carrier-gas flow rate is high. This effect is shown in Table 12. At the higher flow rates, recombination was not significant, and regeneration was more complete in the same residence time. However, under these conditions, an off-gas stream with a high concentration of SO_2 is not obtained. Production of a concentrated SO_2 stream requires that recombination be minimized, regardless of the type of regeneration reactor used. It should be an objective in regenerator design to cause the SO_2 stream to flow past any lower-temperature solids rapidly enough to prevent recombination or else to separate the gas from the solids at a high temperature.

Table 12. Regeneration at 1040°C of Spent Limestone Sorbent in a Small Rotary Kiln

Sample	Carrier-Gas Flow, L/min	Sulfate Conversion to Oxide, %	Sulfate Conversion to Sulfide, %
780522	0.5	33	5
780523	1.0	55	6
780525	1.0	64	18
780621	1.0	19	48 ^a

^aExcess carbon in the feed--i.e., 1.5 times stoichiometric.

TASK D. EFFECTS OF LIMESTONE SULFATION ACCELERATORS ON
CORROSION RATES OF METALS IN AN AFBC

1. Atmospheric Combustor Facility for Corrosion Tests
(J. Lenc, G. Smith, F. G. Teats, and R. Mowry)

This work to study the effects of limestone sulfation accelerators on corrosion rates of metal components of an AFBC is related to a laboratory-scale investigation to increase the degree of sulfation of partially sulfated lime solids within a fluidized-bed combustor by means of additives (*i.e.*, sulfation accelerators). Sulfation accelerators such as NaCl, CaCl₂, and Na₂CO₃ added in small amounts to the lime solids increase both the rate and the extent of sulfation for many limestones.¹

Increased SO₂ capacity of limestone would mean a decrease in the quantity of lime solids required for the combustion process. Such a decrease in the lime solids requirement would lower the process cost and reduce the environmental impact of solids waste disposal. However, there is concern that volatilization of these sulfation accelerators (alkali metal compounds) might cause unacceptable corrosion of the metal components of the combustion system. A separate laboratory-scale investigation of the corrosiveness of salts mixed with sulfated limestones is in progress.¹ The following section of this report (section 2) summarizes corrosion experiments done to date in laboratory-scale apparatus.

a. Description of Atmospheric Combustor Facility for Corrosion Tests

To measure the corrosion rates of metals of construction in the presence of sulfation accelerators in a PDU-scale unit, a new automated atmospheric-pressure fluidized-bed coal combustion facility (AFBC) was designed and constructed. Major components of this new facility are an air preheater, an atmospheric combustor, coal and limestone-sorbent hopper-feeder assemblies, two parallel off-gas particulate-removal systems (each system consisting of two cyclones and a sintered-metal final filter) and an off-gas analysis system. Figure 5 is a simplified piping schematic of the new facility. A schematic diagram of the 152-mm-ID atmospheric combustor to be used in the new facility is shown in Fig. 6. Figure 7 is a photograph showing some major components of the new facility.

The AFBC was designed for attended operation one shift per day and automated operation on the remaining two shifts. Details of the process control system for automated operation are discussed in the following section. Anticipated nominal operating conditions for combustion are listed in Table 13.

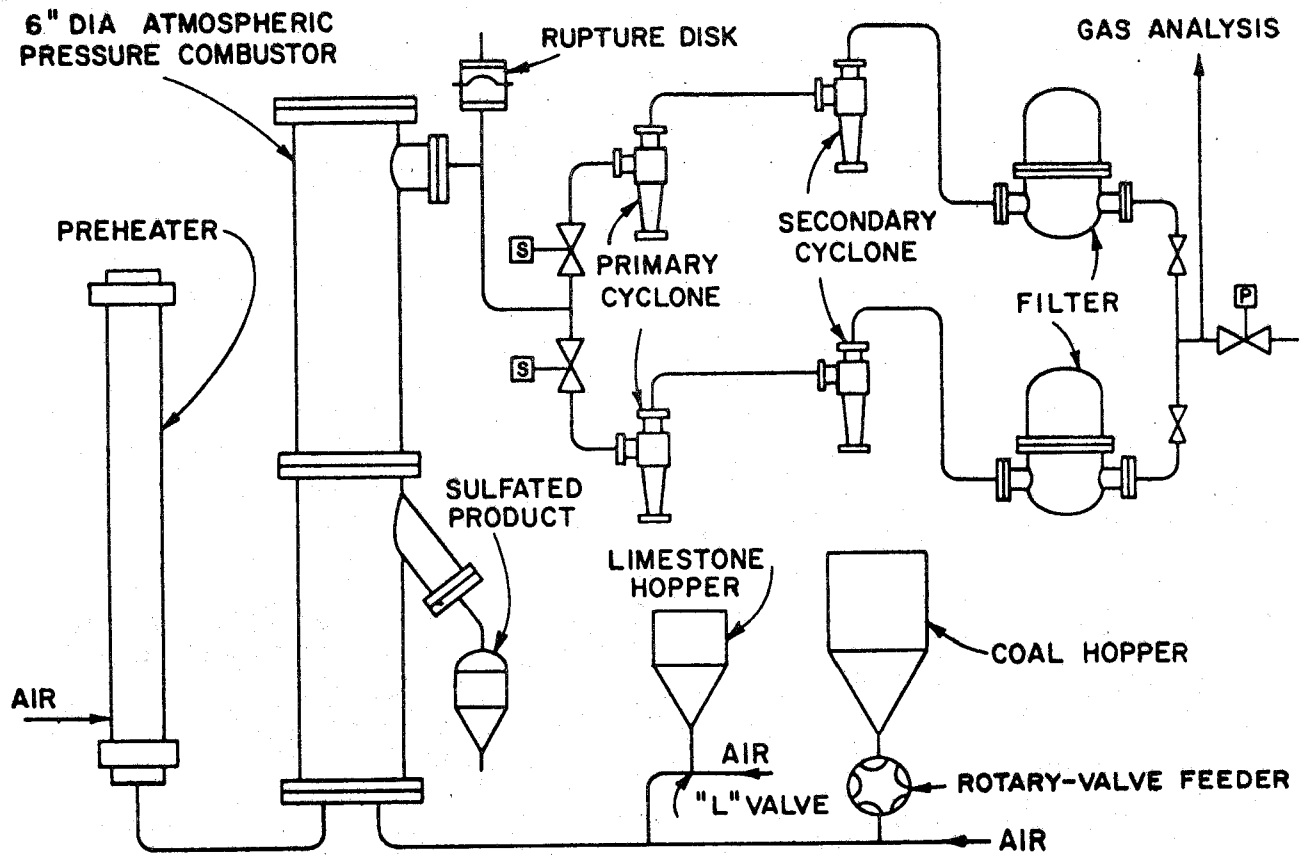


Fig. 5. Simplified Piping Schematic of Atmospheric Combustor Facility

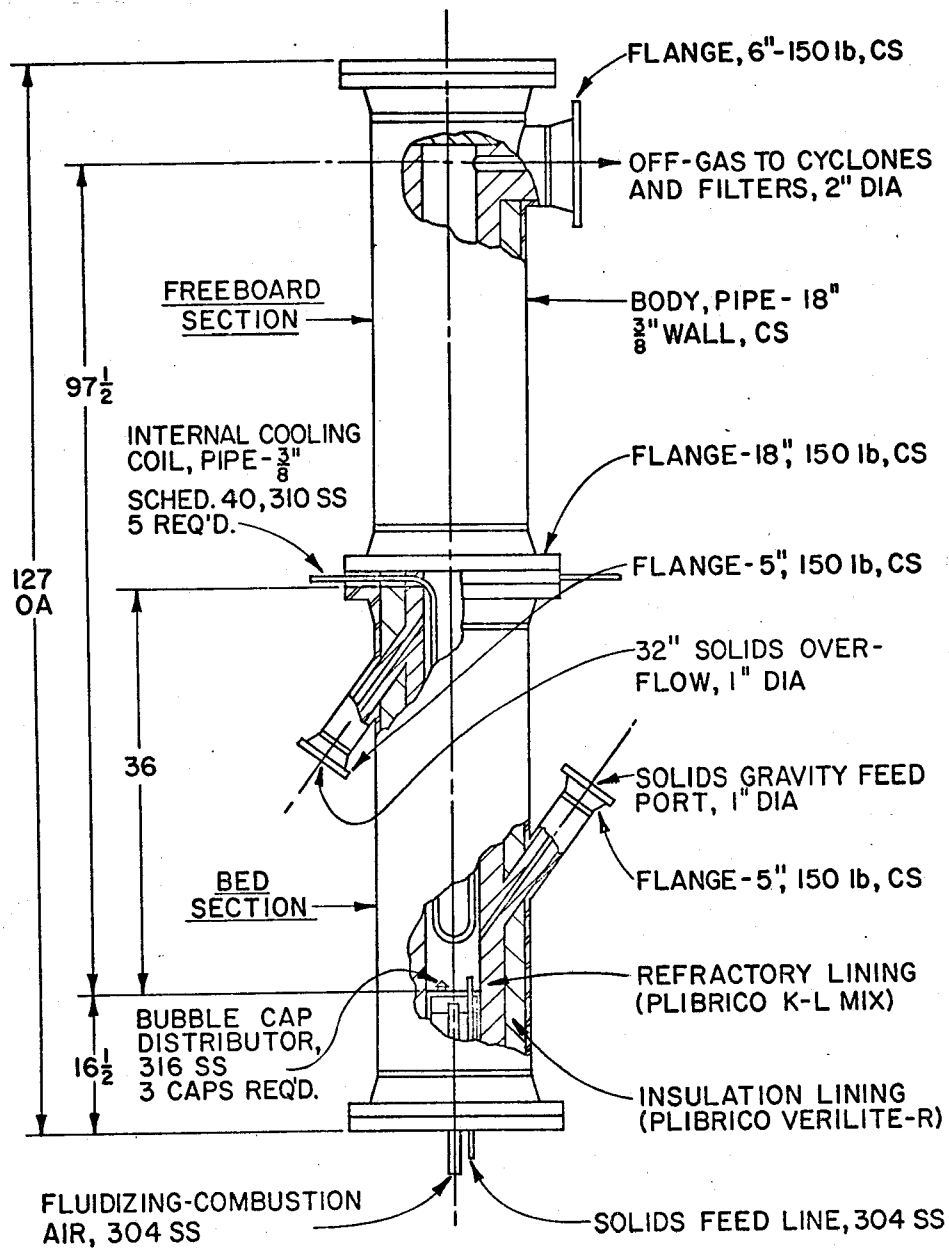


Fig. 6. 152-mm-ID Atmospheric Combustor.
Pipe and flange sizes (nominal sizes) are American standard.

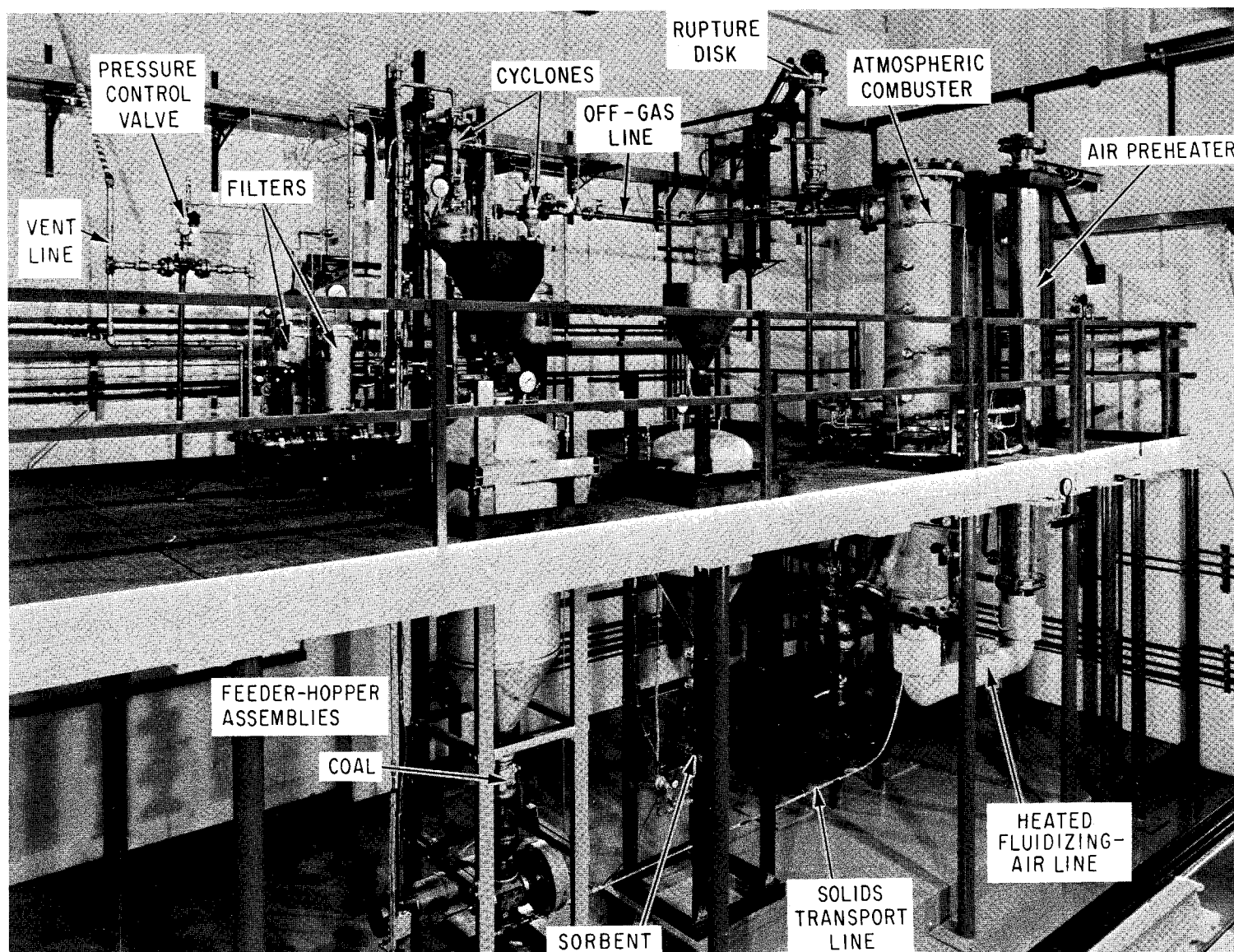


Fig. 7. Some Major Components of the New AFBC.
ANL Neg. No. 308-78-63A

Table 13. Nominal Operating Conditions. Atmospheric Fluidized-Bed Combustor.

Process Variable	Nominal Value
Fluidized-Bed Temperature	855°C (1571°F)
Pressure	152 kPa (1.5 atm)
Superficial Fluidizing Gas Velocity	1 m/s (3.3 ft/s)
Coal Feed Rate ^a	895 mg/s (7.1 lb/h)
Limestone Feed Rate ^b	428 mg/s (3.4 lb/h)
Heat Generation Rate	26.3 kJ/s (89,800 Btu/h)
Fluidized-Bed Height	813 mm (32 in.)
Fluidizing-Combustion Air Flow Rate	6800 cm ³ /s (14.4 scfm)
Estimated Coolant Air Required	18900 cm ³ /s (40 scfm)

^aBased on eastern bituminous coal, such as Sewickley.

^bBased on Greer limestone. Ca/S mole ratio = 3.

b. Automatic Operation of the AFBC Corrosion Test Facility

The fluidized-bed corrosion test facility is designed for fully automatic unattended operation. The process control system is nearly complete, and engineering evaluation will be possible after a few minor alterations. These engineering evaluations will consist of a short series of continuously attended, 100-h runs to determine the reliability of the automatic control system. Based on the results of these evaluations, any necessary changes for automatic unattended operation will be implemented and tested.

A large portion of the automatic instrumentation provides analytical data about the process. Upstream from the instruments for analyzing gaseous constituents in the off-gas, a portion of the gas is passed through a gas-conditioning system in which the off-gas is dried and the sample-gas flow is regulated. The dried off-gas is then distributed via a manifold to various gas analyzers. Infrared analyzers provide continuous analysis for CO, CH₄, H₂O, and CO₂ concentrations. In addition, O₂ is monitored by a paramagnetic analyzer, total hydrocarbons by a flame-ionization analyzer, SO₂ by a pulsed fluorescent analyzer, and NO/NO_x by a chemiluminescent analyzer.

In addition to conditions monitored by the analytical instrumentation, a number of process conditions are monitored. These process variables are controlled with a separate control loop for each variable. The six control loops implemented are shown in Fig. 8 and are described in Table 14.

In addition to the six process-control loops, a relay and timer sequence is used to route off-gas through one of two parallel particulate-removal systems (primary and secondary cyclones and a filter) or through both of them. If an excessive pressure drop occurs across a particulate-removal system, the off-gas flow is switched to the other system and the first is taken out of service. If after a short period (about 10 min) with the second system operating, the pressure drop remains excessive, the first system is

returned to use and both systems are used simultaneously. A continued high pressure drop through both systems for a period of about 10 min would initiate automatic shutdown.

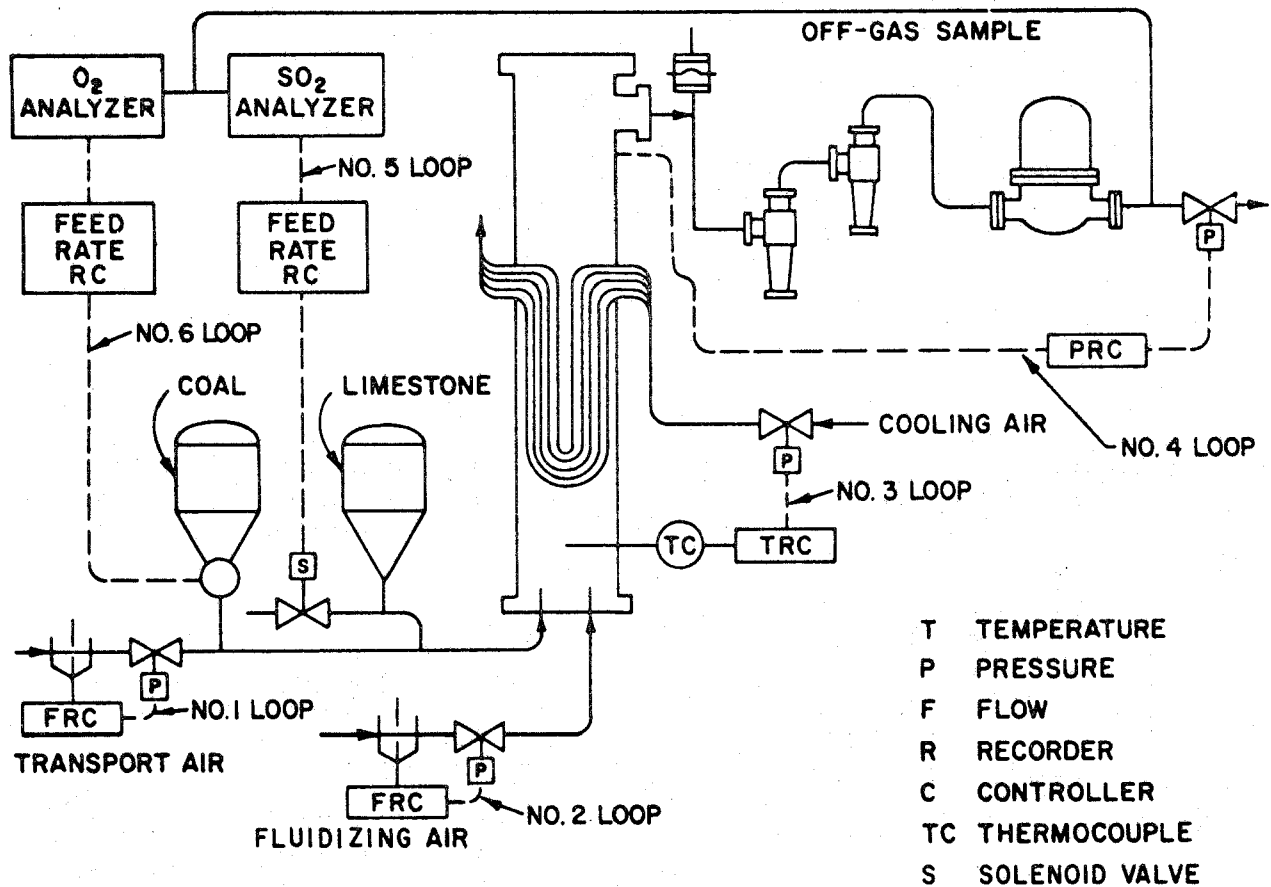


Fig. 8. Automatic Control Loops for Atmospheric Combustor Facility

Experimental operation of the AFBC is monitored and data are recorded by an Acurex Autodata 9 data logger with alarm capabilities. The alarm capabilities can initiate process shutdown in case of a major process upset. As currently set up, the data logger can check any one of 400 channels against high or low limits and for a faulty sensor. During continuous alarm scanning, each channel is tested approximately once every three minutes. However, faster scanning (every 20 s) is possible with some slight loss of accuracy. Fast alarm scanning will be used, and experimental data will be recorded once every 10 min in our experiments.

Table 14. Control Loops for Atmospheric Fluidized-Bed Combustor

Loop Number	Controlled Variable	Setpoint	Measurement	Manipulated Component or Variable
1	Transport air flow rate	2400 cm ³ /s (~5 scfm)	Orifice ΔP	Pneumatic control valve
2	Fluidizing air flow rate	7200 cm ³ /s (15 scfm)	Orifice ΔP	Pneumatic control valve
3	Bed temperature	850°C	Type K thermocouple	Pneumatic control valve (cooling air flow)
4	System pressure	153 kPa (~7.5 psig)	Variable reluctance transducer	Pneumatic control valve
5	SO ₂	750-1500 ppm	Pulsed fluorescent SO ₂ analyzer	Sorbent (limestone) feed rate
6	Excess air	17% (3% O ₂ in off-gas)	Paramagnetic O ₂ analyzer	Coal feed rate

Several unusual process conditions necessitating process shutdown for safety considerations are given in Table 15. The automatic shutdown is controlled by a relay and timer sequence which also activates an alarm at the Laboratory Central Surveillance station. Whenever automatic shutdown is initiated, power to the feeders and the air preheater is shut off. In addition, the fluidizing and transport air streams are replaced with house nitrogen; house nitrogen is also used to purge the filter housings and the coal hopper. Finally, a bypass valve around the system pressure control valve is opened to relieve any excessive system pressure.

Table 15. Process Levels Necessitating Shutdown

Limit	Condition	Level Requiring Shutdown ^a
HI	CO in flue gas	>1%
HI	CH ₄ in flue gas	>1%
LO	O ₂ in flue gas	<2%
HI	Temperature in bed	>1000°C
HI	Temperature in coal hopper	>75°C
HI	Temperature in filter casings	>100°C
HI	Temperature in cyclone receivers	>100°C
HI	Bed ΔP (e.g., as a result of plugged overflow)	>17 kPa (>2.5 psi)
HI	ΔP across gas cleanup system (independent of the data logger)	>34 kPa (>5 psi)
HI	System pressure	>205 kPa (>15 psig)
HI	Temperature of cooling gas outlet manifold	>300°C
LO	Pressure of house high-pressure air supply	<239 kPa (<20 psig)
LO	Flow rate of fluidizing air	<2400 cm ³ /s (<5 scfm)
LO	Flow rate of transport air	<900 cm ³ /s (<2 scfm)
LO	System pressure (e.g., as a result of rupture disc breakage)	<136 kPa (<5 psig)
LO	Pressure of emergency nitrogen supply	<239 kPa (<20 psig)
HI	SO ₂ in flue gas	>1000 ppm
HI	O ₂ in flue gas (air leak into sample system)	>7%

^aTentative levels. To be reevaluated on the basis of actual experimental data.

After an adjustable delay of 10 to 60 min, steps are taken to conserve nitrogen. If the data logger alarm scan indicates that temperatures in key locations are below a predetermined level, the fluidizing and transport gas streams are switched back to air; also, the nitrogen purges of the filter housings and coal hoppers are shut off.

To avoid operating without sufficient nitrogen for emergency shutdown, a slightly different shutdown process is initiated when the pressure of house nitrogen is low. In the latter case, the power to the feeders and the gas preheater is shut off and the bypass valve around the system pressure

control valve is opened. This sequence safely shuts down the system in the event that insufficient nitrogen is available for emergency shutdown. In the latter case, operation is not allowed to continue because the emergency shutdown sequence would be inoperative due to the low supply of purge nitrogen.

c. Planned Schedule for Corrosion Experiments in AFBC

Compositions and geometries of corrosion specimens, as well as preferable locations of exposure in the AFBC, have been selected by O. Chopra of the Materials Science Division of ANL. Parameters to be measured during corrosion tests have been identified.

Initially, to obtain baseline corrosion data on a variety of metals, corrosion combustion experiments are to be made with no sulfation accelerator present in the fluidized bed. Next, 100-h scoping tests will be conducted to determine the possible corrosive effects of a sulfation accelerator on a variety of metal corrosion specimens. The accelerator for these 100-h tests will be selected on the basis of information obtained in laboratory-scale tests. After the 100-h tests, metals and accelerating agents selected for further testing will be subjected to 1000-h tests.

d. Preliminary Runs in the AFBC

A series of runs was carried out in the AFBC (prior to corrosion experiments) to evaluate the effects on SO₂ retention by Grove limestone (1359) of adding low concentrations (1.0 mol % or less) of CaCl₂ or NaCl. In this series of runs, Sewickley coal (either -6 +100 mesh or -12 +100 mesh) was combusted at a bed temperature of 850°C, a pressure of 101.3 kPa (1 atm), a fluidizing-gas velocity of 1 m/s, and a fluidized-bed height of 813 mm, with 3% O₂ in the dry off-gas. The above variables were maintained at the stated values in all runs; only the composition of the limestone sorbent and the Ca/S mole ratio were varied. Grove limestone (-10 +30 mesh), with or without CaCl₂ or NaCl addition, was the sorbent used in this experimental series.

A total of 23 runs were made in which the Grove limestone sorbent contained nominal concentrations of 0, 0.1, 0.3, or 0.5 mol % CaCl₂. Eight additional runs were completed in which the Grove limestone sorbent contained nominal concentrations of 0.5 or 1.0 mol % NaCl.

Analytical data for this series of runs are incomplete. Consequently, the effects of CaCl₂ or NaCl on SO₂ retention by Grove limestone are yet to be evaluated.

2. Corrosion Behavior of Materials in Fluidized-Bed Environments
(J. Shearer, O. K. Chopra,* and C. Turner)

As part of the study of the effects of NaCl and other salts on limestone sulfation, corrosion experiments with several metal alloys were performed to evaluate the corrosiveness of salts in a simulated flue-gas environment. The major component of the experimental apparatus was a 5-cm-ID quartz fluidized-bed vessel (Fig. 9). The bed material consisted of either a batch of fully sulfated dolomite to which particulate salt was added or a continuous feed of raw limestone or dolomite impregnated with salt from an aqueous solution. The compositions of the materials tested are given in Table 16.

* Materials Science Division.

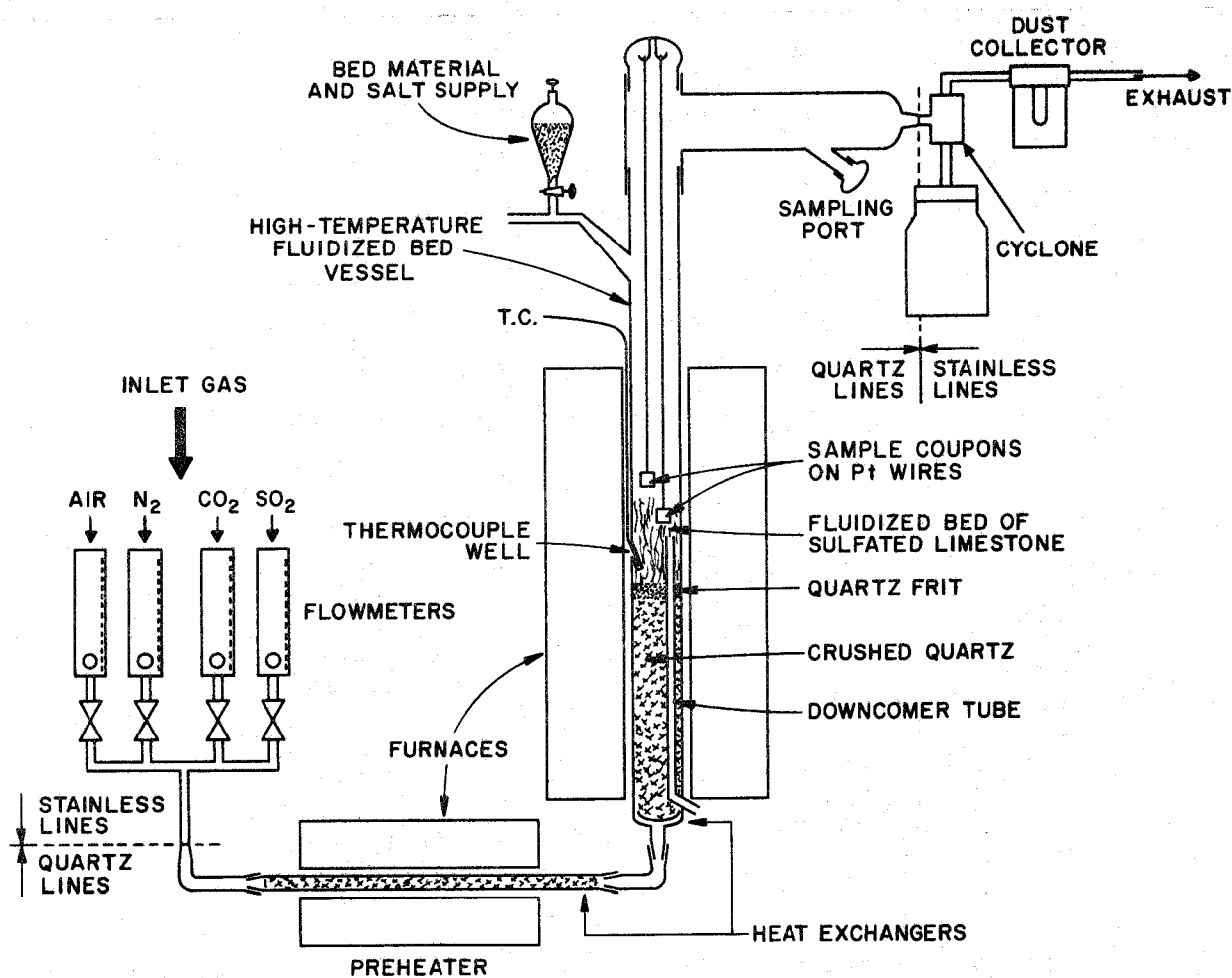


Fig. 9. High-Temperature 5-cm-dia Quartz Fluidized-Bed Reactor for Salt Corrosion Studies

Table 16. Compositions of Alloys (in wt %)

Alloy	Fe	Ni	Cr	Mo	Mn	Si	C	Other Elements
Inconel 600	8.0	Bal.	15.5	—	0.5	0.25	0.08	
Inconel 601	14.1	Bal.	23.0	—	0.5	0.25	0.05	1.35 Al, 0.25 Cu
RA 333	18.0	Bal.	25.0	3.0	1.5	1.25	0.05	3.0 Co, 3.0 W
Type 304 SS	Bal.	9.5	19.0	—	2.0	0.50	0.08	
Type 316 SS	Bal.	12.0	17.0	2.5	2.0	0.50	0.10	
Type 310 SS	Bal.	20.5	25.0	—	2.0	1.50	0.25	
Type 321 SS	Bal.	10.5	18.0	—	2.0	1.00	0.08	0.40 Ti
Incoloy 800	Bal.	32.5	21.0	—	1.5	1.00	0.10	0.38 Al, 0.38 Ti
9Cr-2Mo	Bal.	—	9.5	2.1	0.9	0.33	0.09	

Corrosion coupons were suspended on platinum wires, both within and above the fluidized-bed material at 850°C (1123 K) for 100 h. The bed materials and the fluidizing-gas compositions for the various tests are listed in Table 17. For batch runs, NaCl was injected as a solid powder

Table 17. Experimental Conditions

Run	Bed Material	Fluidizing-Gas Composition
1	Fully sulfated dolomite	5% O ₂ , 200 ppm SO ₂ , balance N ₂
2	Fully sulfated dolomite, 1.5 g solid NaCl introduced every 4 h	5% O ₂ , 200 ppm SO ₂ , balance N ₂
3	Dolomite treated with NaCl (3.0 mol % NaCl)	5% O ₂ , 3200 ppm SO ₂ , balance N ₂
4	Limestone treated with CaCl ₂ (0.1 mol % CaCl ₂)	5% O ₂ , 3200 ppm SO ₂ , balance N ₂
5	Dolomite treated with NaCl (1.0 mol % NaCl)	5% O ₂ , 3200 ppm SO ₂ , balance N ₂

into the bed from above (run 2). In runs 3, 4, and 5, salt was introduced in pretreated dolomite or limestone, prepared by soaking the stone in a salt solution and drying. Small portions of the treated stone were periodically introduced into the fluidized bed. The fluidized-bed vessel was equipped with an overflow tube which maintained a constant bed level. For these runs, the fluidizing gas contained 3200 ppm SO₂. After reacting with the bed material, the fluidizing gas contained 200-500 ppm SO₂, 5% O₂, and the balance N₂ and flowed at approximately 0.9 m/s.

Metallographic examinations (in the Materials Science Division of this Laboratory) were performed on corrosion specimens, some exposed to beds with salt and some exposed to beds without salt.

a. Metallographic Examination

The corrosive attack on all specimens was primarily oxidation, with some sulfidation of the material. In general, the addition of salt to the fluidized bed increased the corrosion rates. The average thicknesses of the surface scales and the depths of corrosion-product penetration for the specimens exposed inside and above fluidized beds are shown in Figs. 10 and 11, respectively. In the absence of salt, all materials developed 2- to 3- μ m-thick surface scales when exposed either above or in the fluidized bed which contained sulfated dolomite. The corrosive attack under the surface scale in these specimens was minimal. However, under the same environmental conditions, Inconel 601 specimens suffered considerable internal attack because the exposure temperature was about 50 K higher, i.e., about 1173 K.

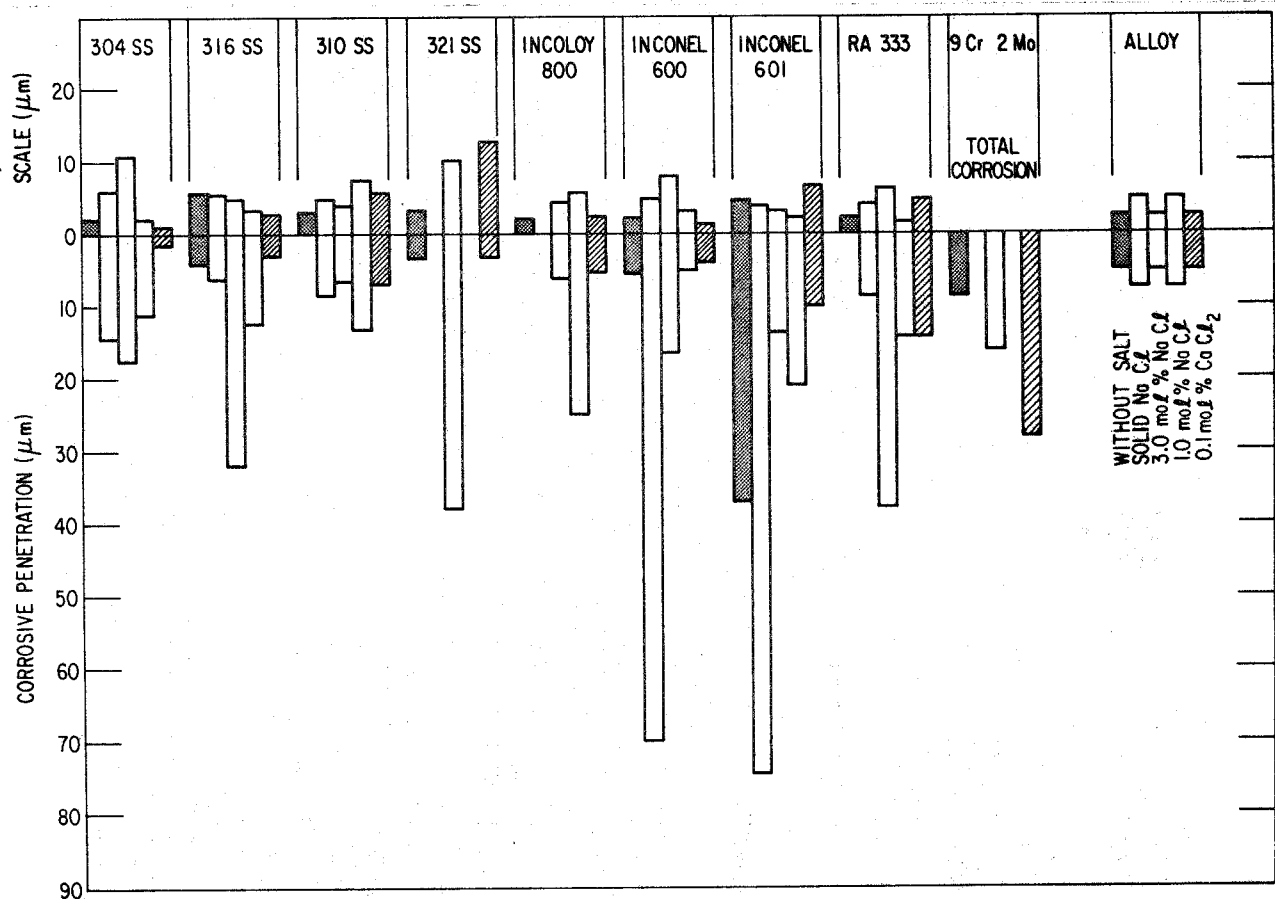


Fig. 10. Average Thickness of Surface Scale and Corrosive Penetration for Corrosion Coupons Exposed Inside the Bed for 100 h at 1123 K except that the Temperature for Inconel 601 was 1173 K.

As shown in Figs. 10 and 11, the addition of salt to the fluidized bed increased the corrosive attack on all materials. The iron-base alloys, (namely, Types 304, 316, and 310 stainless steel) fared better than the high-nickel alloys. For these stainless steels, a variation in the amount of NaCl in the bed had little or no effect on their corrosion behavior. In the presence of NaCl, the average value of the total corrosive attack, *i.e.*, the scale thickness plus the depth of penetration, observed in Types 304, 316, and 310 stainless steel was about 20 μm as compared with about 4 μm in the absence of salt and about 8 μm in the presence of 0.1 mol % CaCl_2 .

The corrosion behavior of the nickel-base alloys, *i.e.*, Inconel 600, Inconel 601, and RA333, showed a dependence on the amount of salt in the fluidized bed. The addition of solid NaCl (run 2) increased the corrosive attack drastically, *i.e.*, thick surface scales formed and extensive internal attack occurred. The specimens exposed above the bed generally showed greater corrosive penetration than those exposed inside the bed. However, in the presence of 1.0 mol % NaCl or 0.1 mol % CaCl_2 , the corrosion behavior for these alloys was comparable to that of the stainless steels.

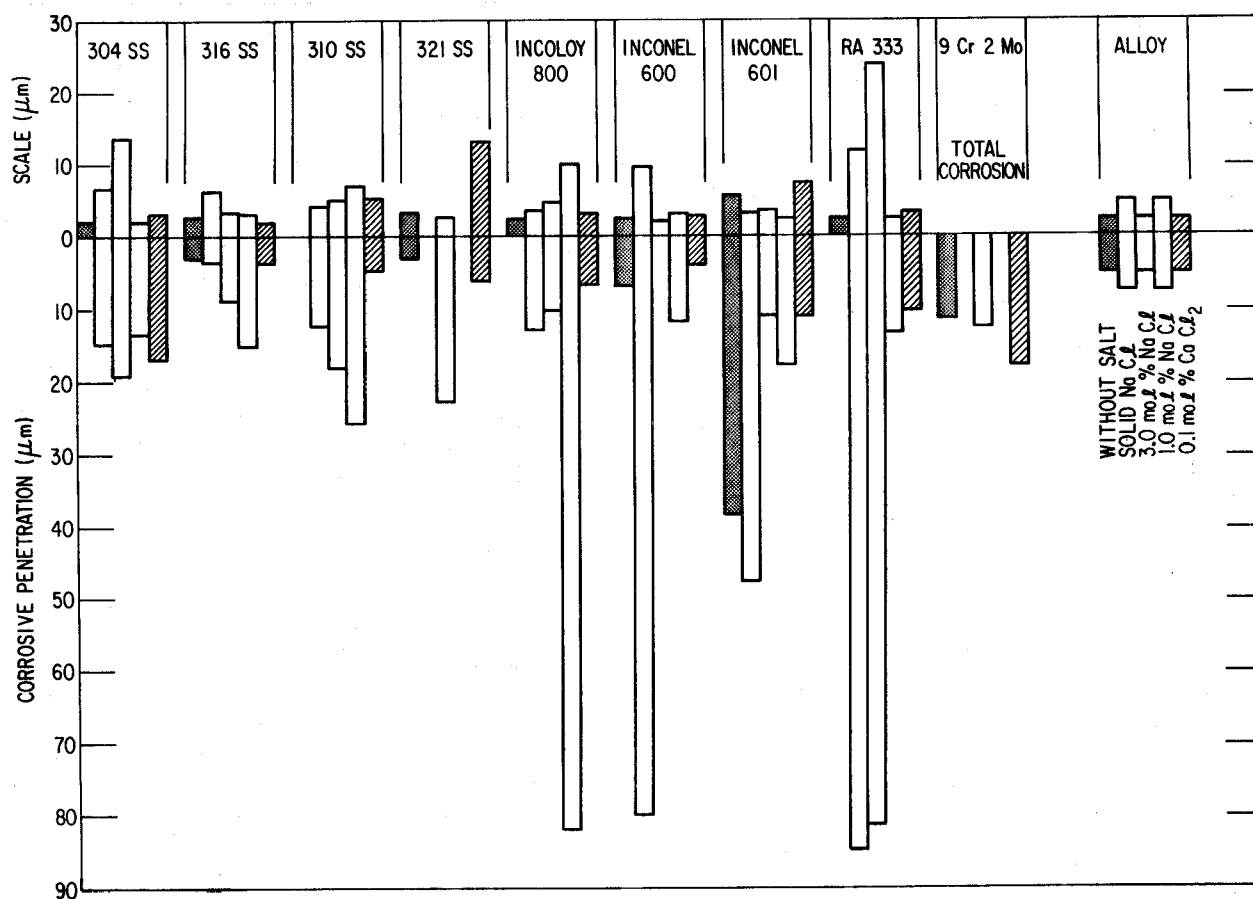


Fig. 11. Average Thickness of Surface Scale and Corrosive Penetration for Corrosion Coupons Exposed Above the Bed for 100 h at 1123 K except that for Inconel 601 the Temperature was 1173 K.

Detailed metallographic examination was made of all the specimens to determine the distribution of corrosion products. Figures 12 to 17 show scanning-electron micrographs (SEMs) of the cross sections of specimens of Types 304 and 310 stainless steel, Incoloy 800, Inconel 600, Inconel 601, and RA333 exposed under various test conditions. The specimens exposed to the environment with NaCl or CaCl₂ exhibited large cavities along the grain boundaries. Micrographs of the specimens indicate that the internal corrosive attack is caused primarily by the preferential oxidation of the carbide phases. Carbon from the carbides diffuses into the material and reprecipitates ahead of the oxidation front, as shown in Figs. 14c and 17b. These specimens showed a depletion of chromium in the surface region. The X-ray microprobe line analyses for nickel, iron, and chromium on Incoloy 800 specimens, which had been exposed above NaCl-containing and NaCl-free bed material, are shown in Figs. 18a and 18b, respectively. In the absence of NaCl, the distribution of nickel, iron, and chromium in the specimen is relatively uniform although some enrichment of chromium occurs at the surface. However, in the presence of NaCl, the surface region is depleted of chromium and iron to a depth of about 60 μm. The specimen matrix in this region consists primarily of nickel.

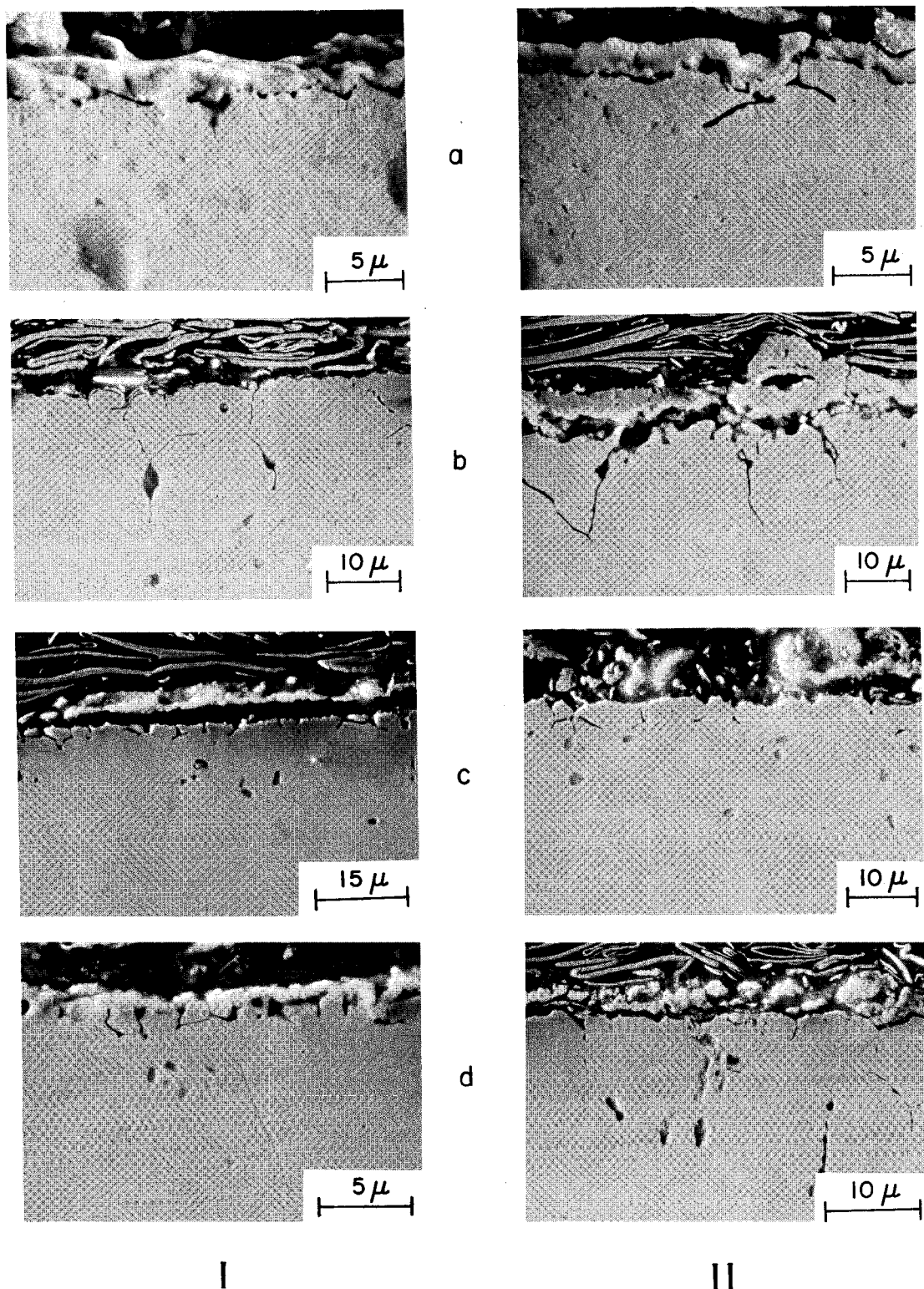


Fig. 12. SEMs of Type 304 Stainless Steel after a 100-h Exposure at 1123 K. (I) Exposed in bed, (II) exposed above bed, (a) without salt, (b) solid NaCl, (c) 1.0 mol % NaCl, and (d) 0.1 mol % CaCl_2 . ANL Neg. No. 306-78-795

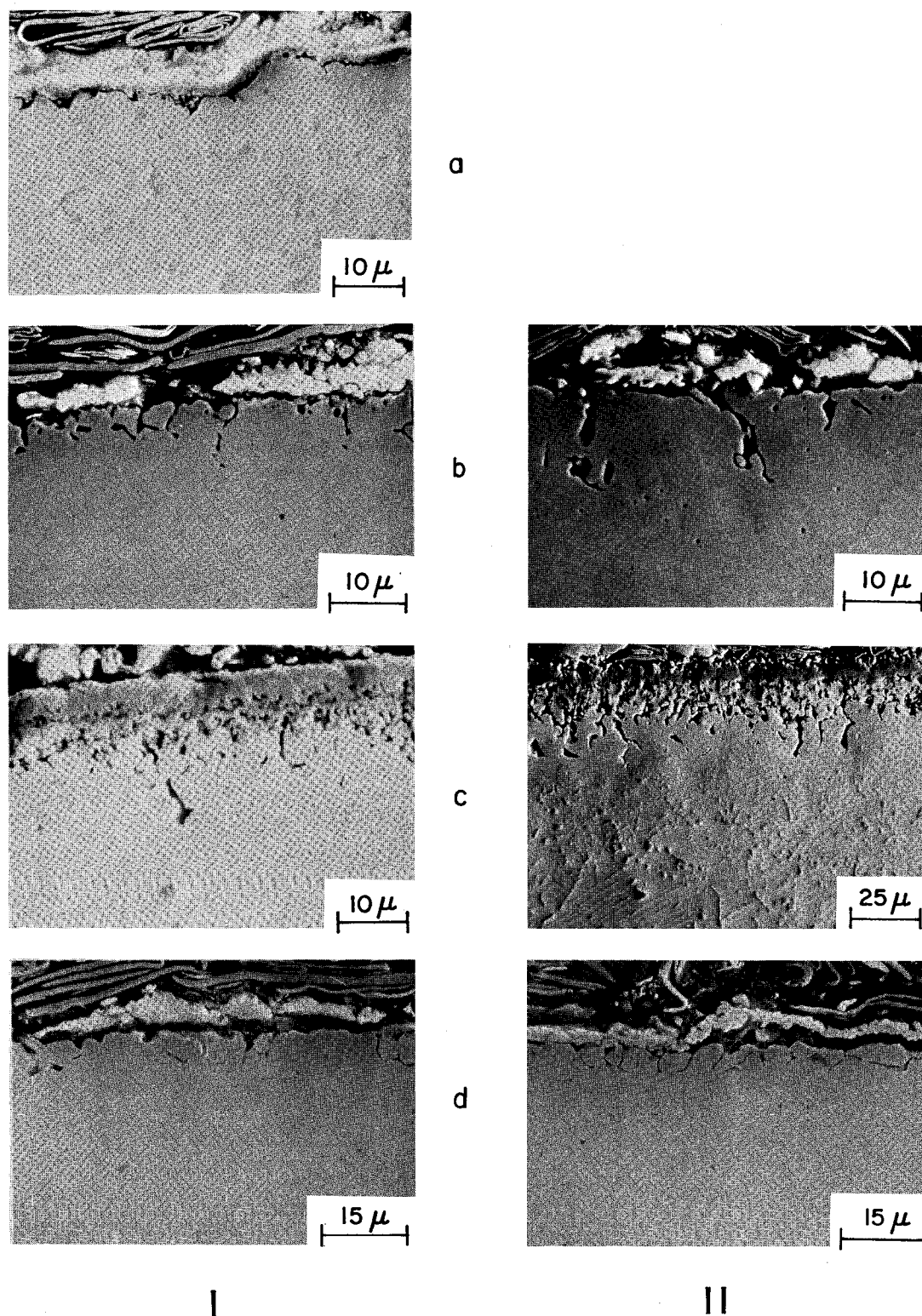


Fig. 13. SEMs of Type 310 Stainless Steel after a 100-h Exposure at 1123 K. (I) Exposed in bed, (II) exposed above bed, (a) without salt, (b) solid NaCl, (c) 1.0 mol % NaCl, and (d) 0.1 mol % CaCl_2 . ANL Neg. No. 306-78-797

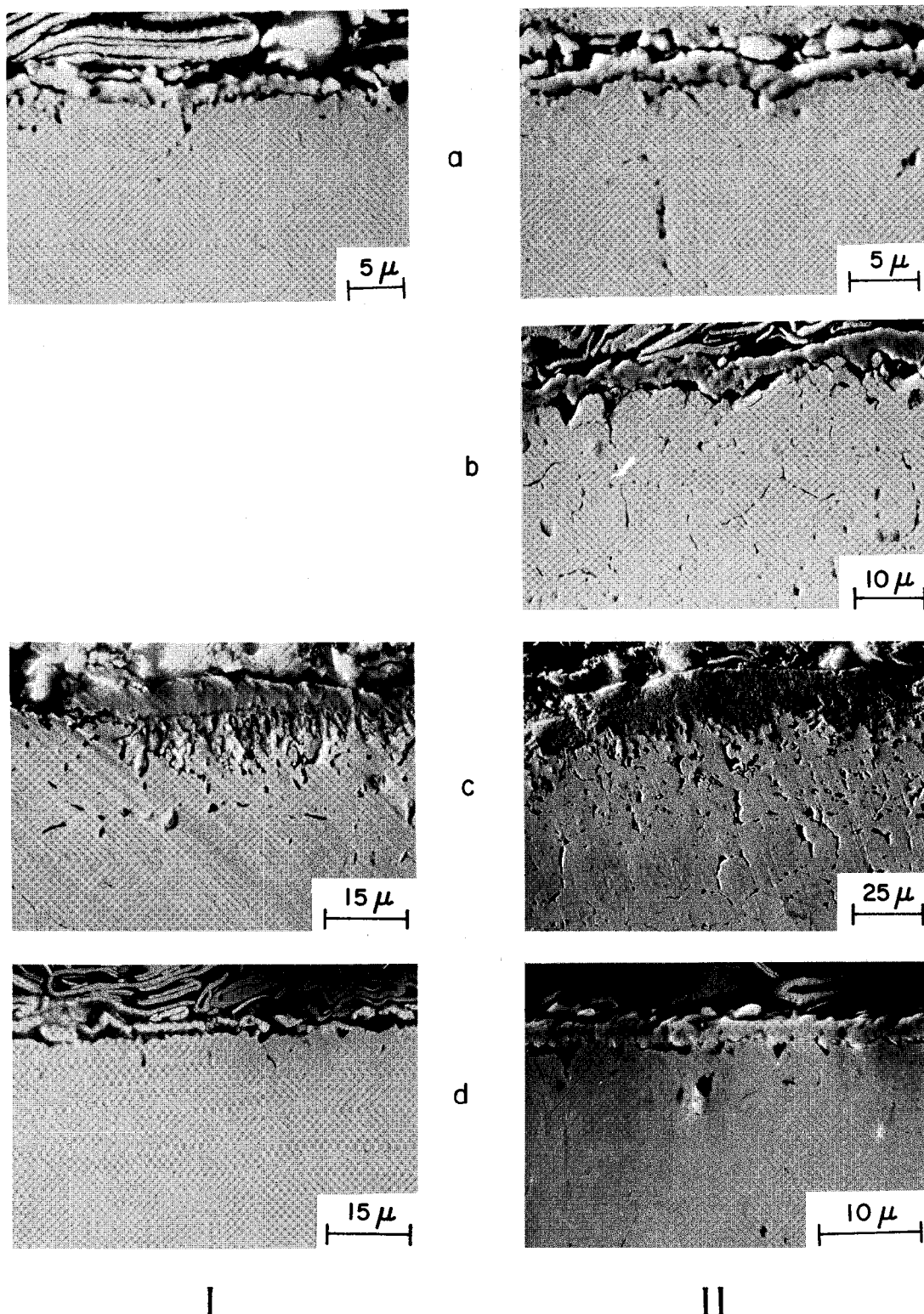


Fig. 14. SEMs of Incoloy 800 after a 100-h Exposure at 1123 K. (I) Exposed in bed, (II) exposed above bed, (a) without salt, (b) solid NaCl, (c) 1.0 mol % NaCl, and (d) 0.1 mol % CaCl_2 . ANL Neg. No. 306-78-798

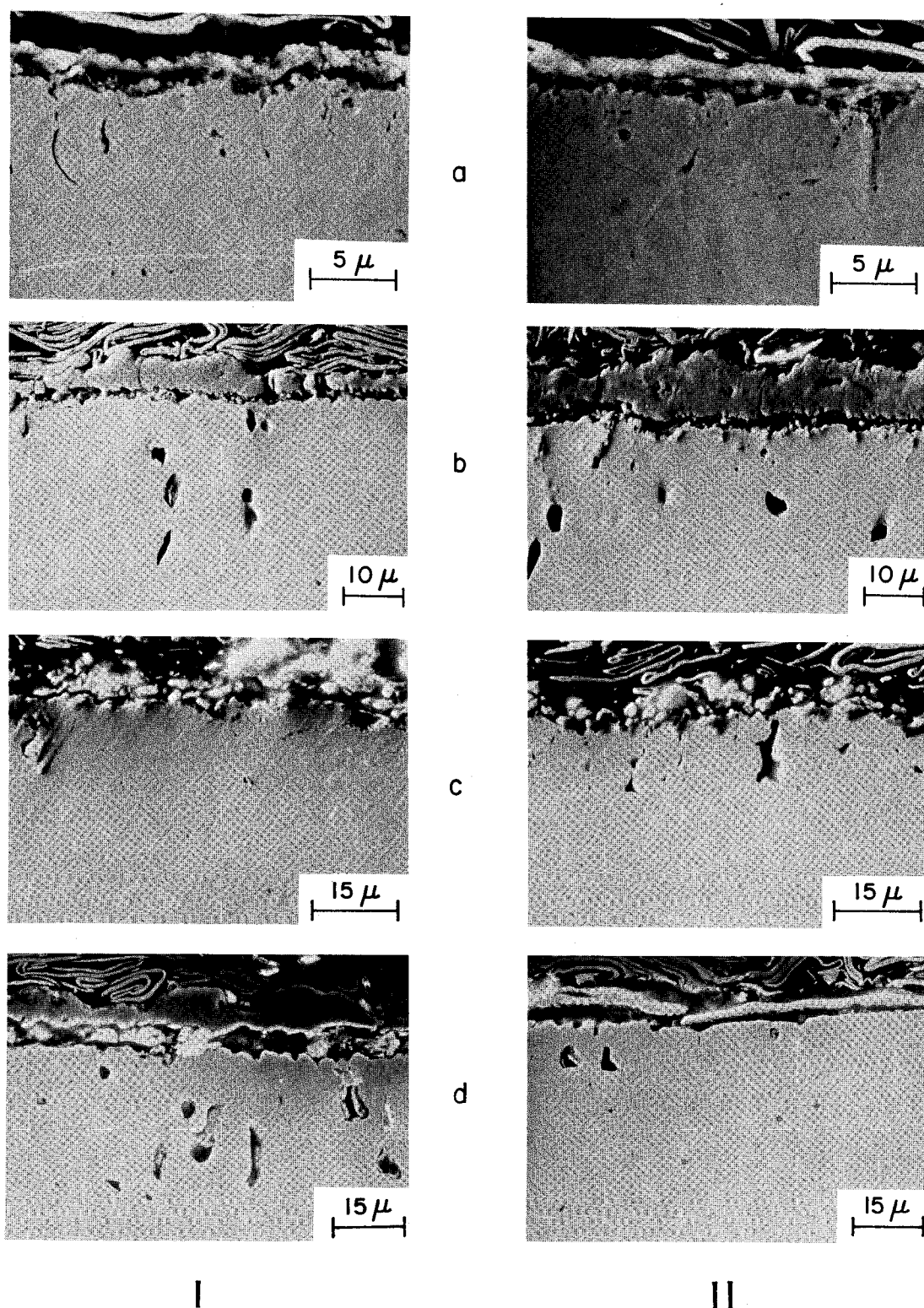


Fig. 15. SEMs of Inconel 600 after a 100-h Exposure at 1123 K. (I) Exposed in Bed, (II) exposed above bed, (a) without salt, (b) solid NaCl, (c) 1.0 mol % NaCl, and (d) 0.1 mol % CaCl_2 . ANL Neg. No. 306-78-796

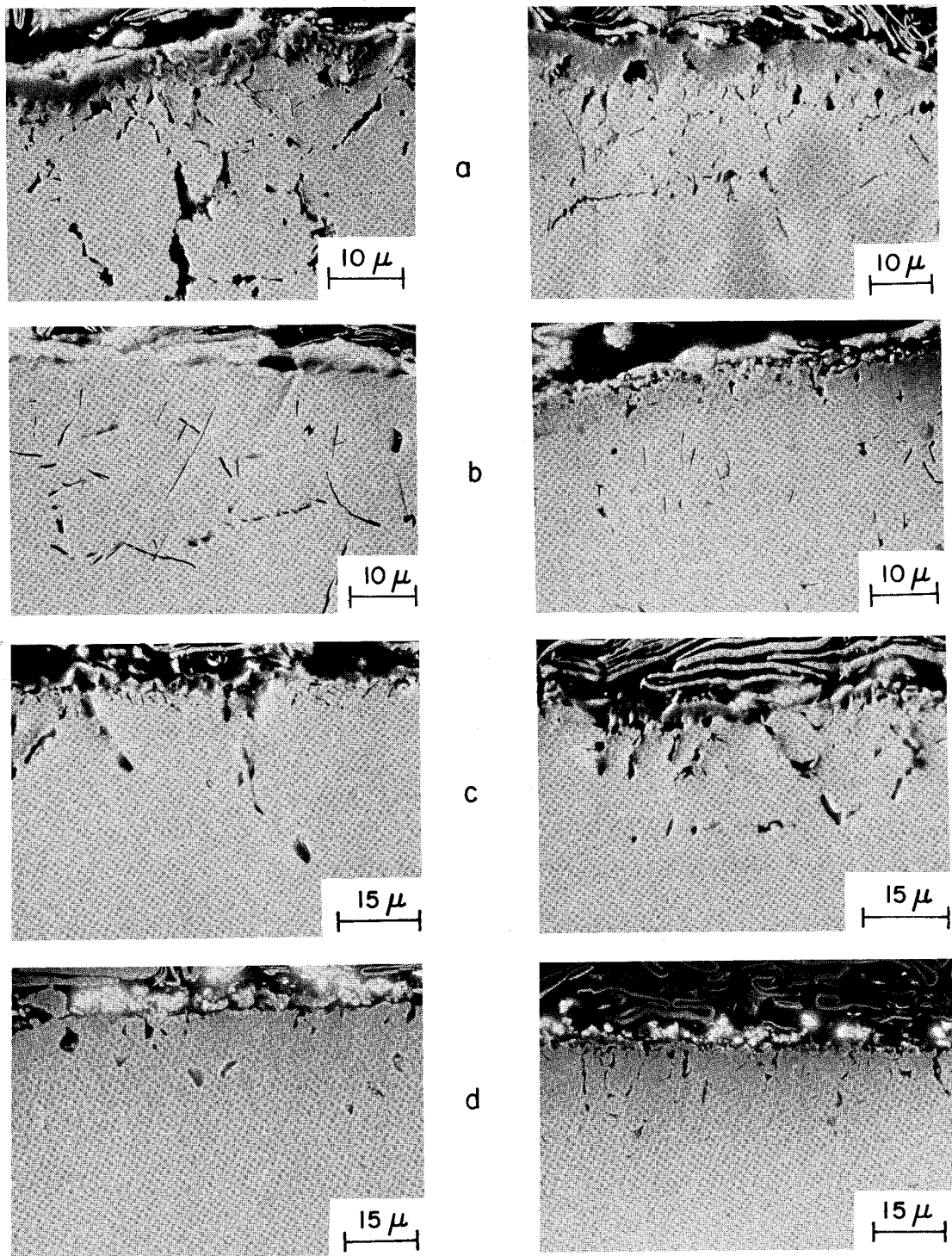


Fig. 16. SEMs of Inconel 601 after a 100-h Exposure at 1123 K. (I) Exposed in bed, (II) exposed above bed, (a) without salt, (b) solid NaCl, (c) 1.0 mol % NaCl, and (d) 0.1 mol % CaCl_2 . ANL Neg. No. 306-78-794

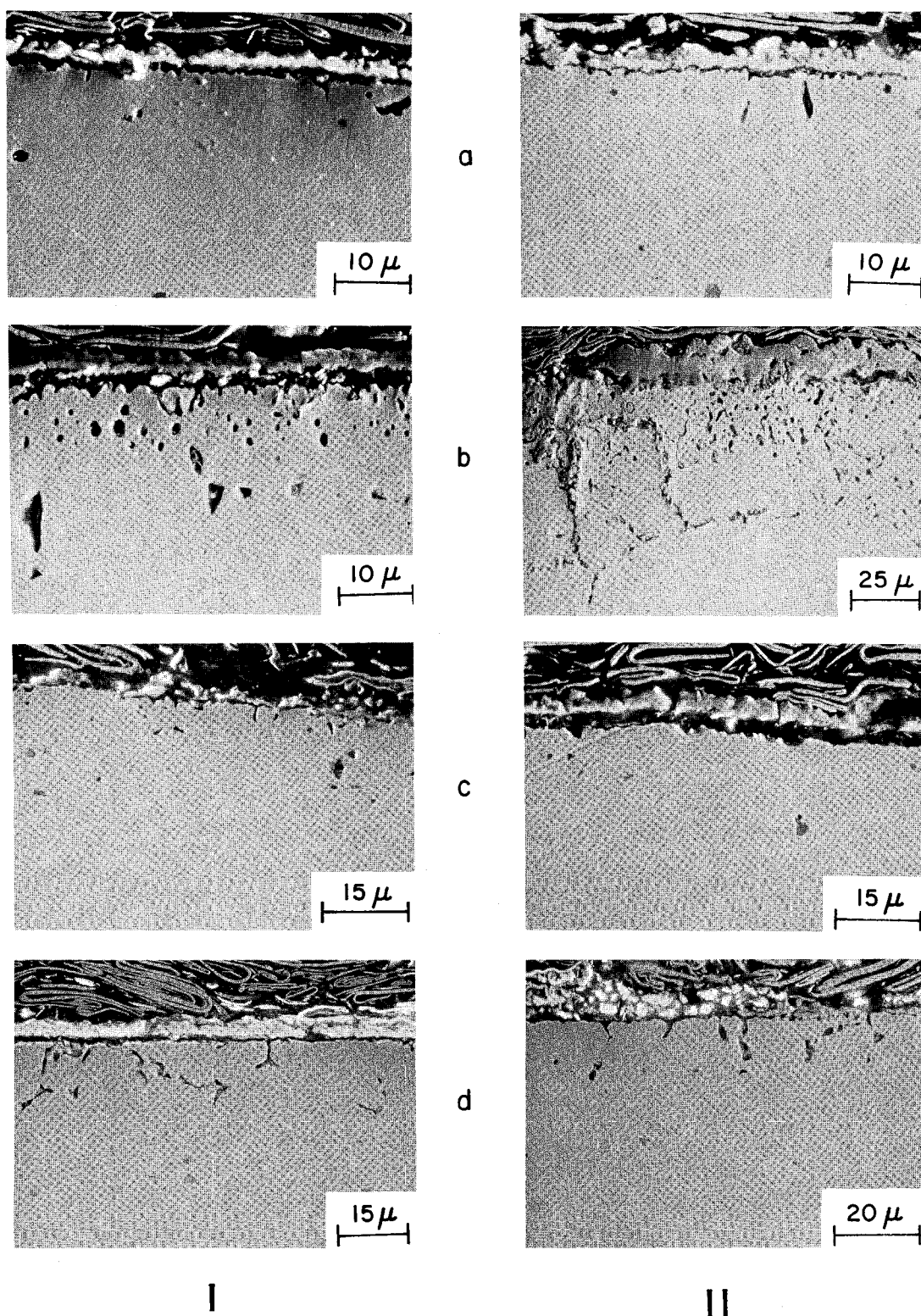


Fig. 17. SEMs of RA333 after a 100-h Exposure at 1123 K. (I) Exposed in bed, (II) exposed above bed, (a) without salt, (b) solid NaCl, (c) 1.0 mol % NaCl, and (d) 0.1 mol % CaCl_2 . ANL Neg. No. 306-78-793

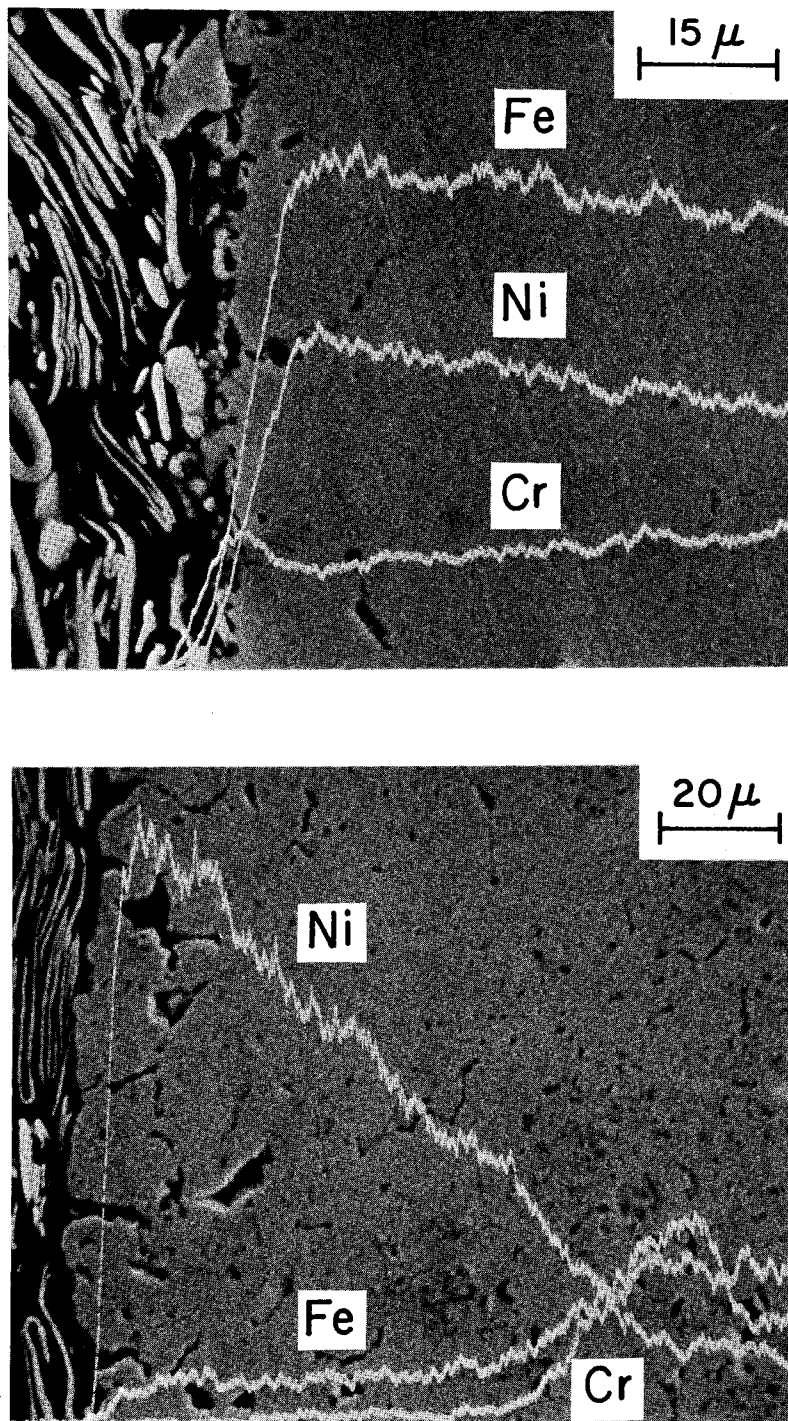


Fig. 18. X-ray Microprobe Line Analyses for Ni, Fe, and Cr on Incoloy 800 Specimens Exposed above the Bed for 100 h at 1123 K.
(a) Exposure above bed without salt and
(b) above bed with solid NaCl added.
ANL Neg. No. 306-78-787

Scanning-electron micrographs and energy-dispersive X-ray (EDAX) analyses of the surface of the scales formed on Incoloy 800 specimens which were exposed above the bed (1) free of and (2) containing NaCl, are shown in Figs. 19a and 19b, respectively. In the absence of NaCl, a continuous oxide scale formed on the specimen surface. The major elements in the scale are chromium, manganese, and iron. Minor amounts of calcium, magnesium, silicon, sulfur, aluminum, and titanium are also observed. Sulfur is probably present

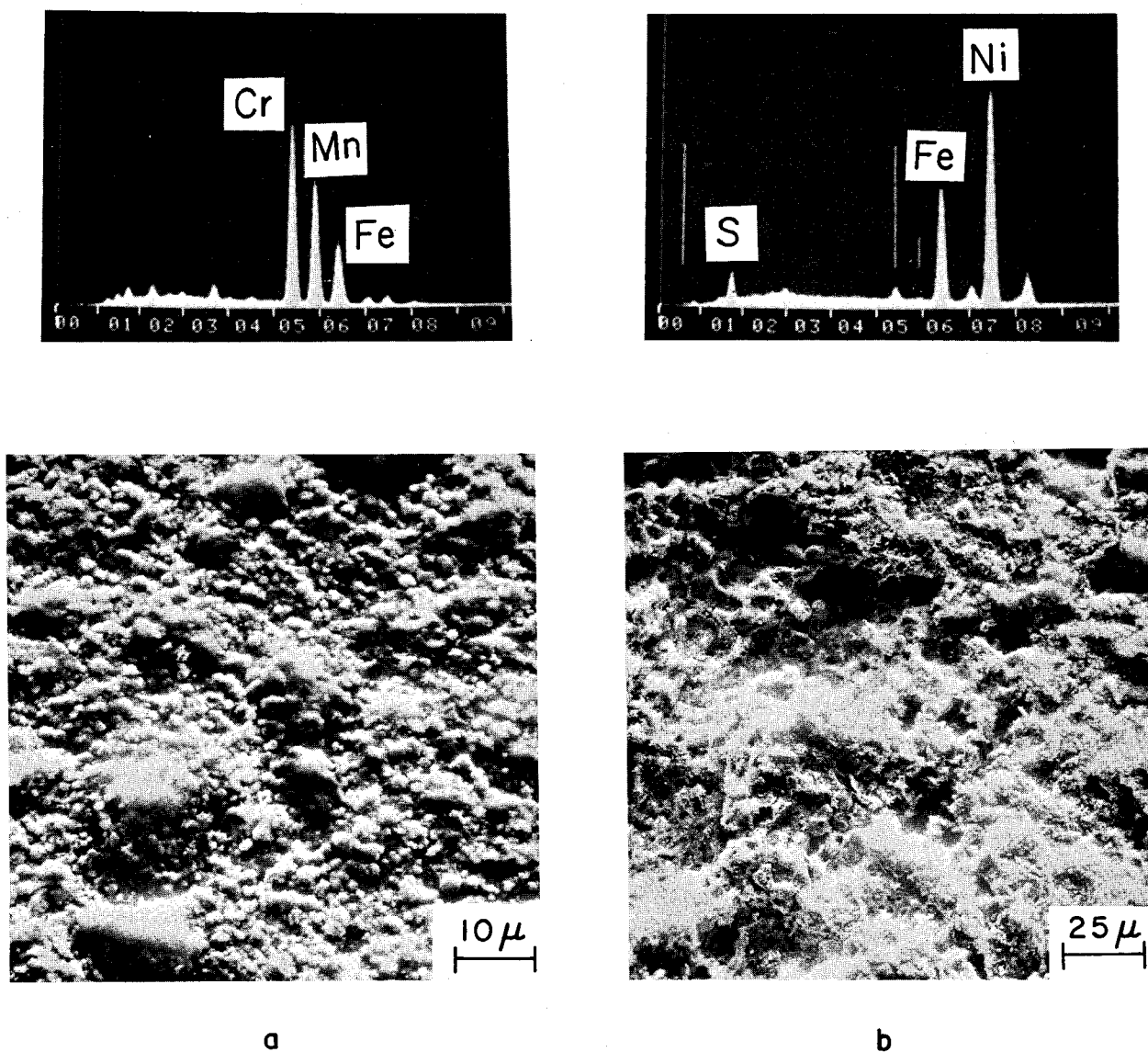


Fig. 19. SEMs and EDAX Analysis of the Surface of the Scales Developed on Incoloy 800 Exposed above the Bed for 100 h at 1123 K.
 (a) Exposure without salt and
 (b) with solid NaCl
 ANL Neg. No. 306-78-458

in calcium sulfate particles that deposit on the scale. When NaCl is present in the bed, the specimen surface is quite corroded, (Fig. 19b) and the metal grains underneath the scale are exposed. The EDAX analysis of the surface shows the presence of nickel, iron, and silicon.

The addition of salt to the fluidized bed also caused internal sulfidation of some of the alloys, e.g., Type 304 stainless steel and RA333 specimens (shown in Fig. 12c and 17c, respectively). The patches of sulfide were always observed in a region between the oxidation front and areas where the carbides reprecipitate.

These results indicate that NaCl causes destruction of the normally protective oxide scales. This process leads to continuous depletion of chromium and iron in the specimen matrix. The absence of a stable and adherent oxide scale leads to internal oxidation and sulfidation of the alloys. The sulfides are always observed ahead of the oxidation front. This behavior shows that diffusion of sulfur in the matrix is faster than diffusion of oxygen.

For most of the alloys, the internal corrosive attack consists of three distinct zones. At the zone near the surface, there is internal oxidation. The matrix is depleted in chromium and shows iron-silicon oxides along the grain boundaries. The second zone consists of patches of chromium and manganese sulfides. In this region, the partial pressure of oxygen is low and chromium reacts preferentially with sulfur to form sulfides. The internal oxidation and sulfidation zones are free of carbide particles. The carbides in these zones are either oxidized or they dissolve and the carbon diffuses into the material and reprecipitates as chromium-rich carbides ahead of the sulfidation zone. The third zone consists of these reprecipitated carbide particles.

b. Effect of Temperature

To evaluate the effect of temperature on the corrosion behavior of materials in the presence of salt, corrosion specimens were placed inside and at different heights above the fluidized bed. The temperature of the specimens varied from 1123 K to 723 K (850 to 450°C). For these tests, the fluidized bed contained 3.0 mol % NaCl. Micrographs of Types 304 and 310 stainless steel specimens exposed inside and above the bed at different temperatures are shown in Figs. 20 and 21, respectively.

The corrosion behavior of the specimens that were exposed inside and above the bed at 1123 K (850°C) is similar to that described in the previous section. However, the specimens exposed above the bed at lower temperatures show considerably more corrosive attack. The total depths of corrosion in Types 304 and 310 stainless steel specimens at 923 K (650°C) are 80 and 50 μm , respectively, and at 823 K (550°C) the values are 600 and 100 μm , respectively. At these temperatures, the surface scales consist of an outer layer of iron oxide with an inner layer of mixed oxides of iron and chromium. The alloy matrix shows extensive internal sulfidation and oxidation.

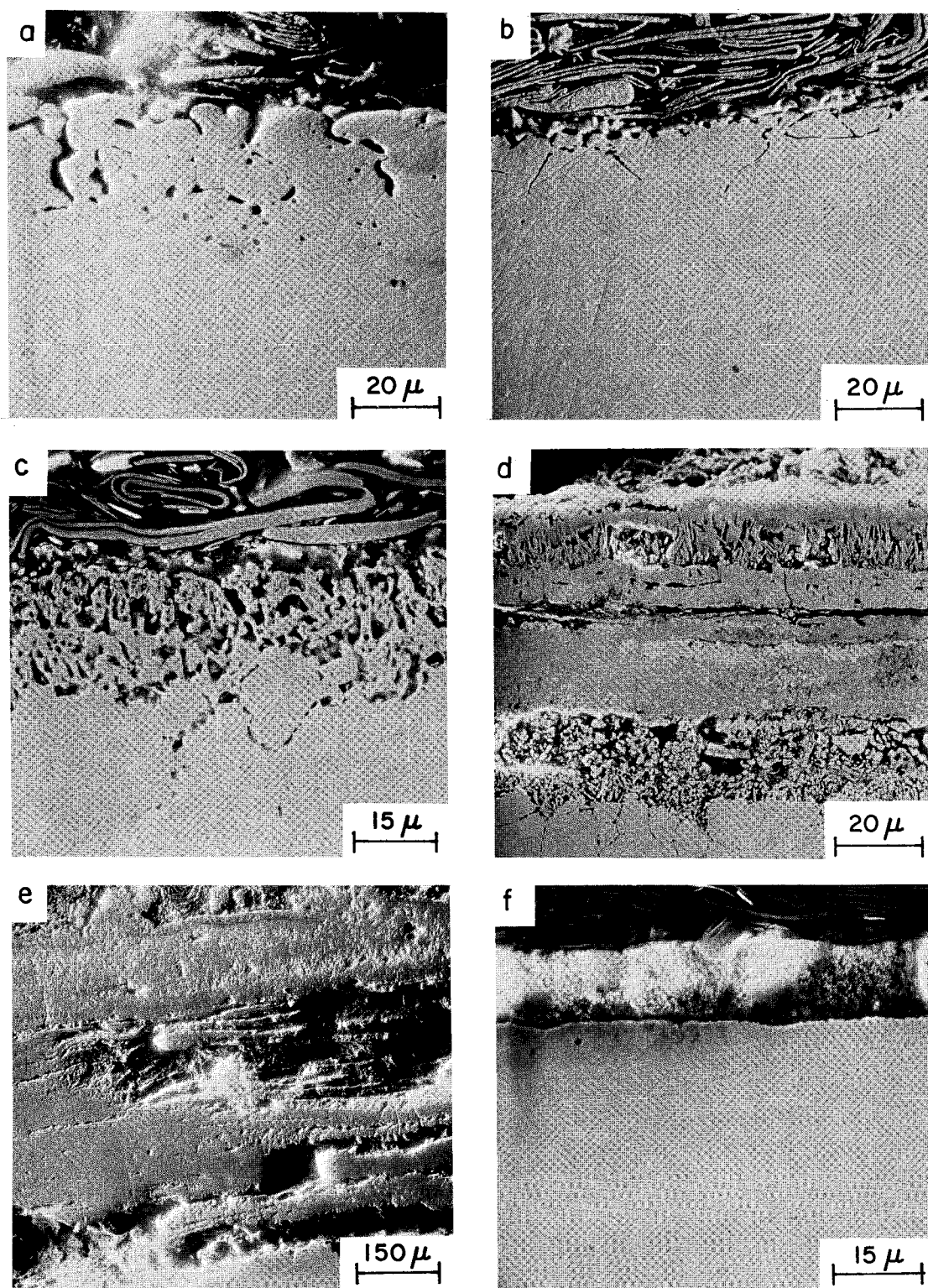


Fig. 20. SEMs of Type 304 Stainless Steel after a 100-h Exposure. (a) Exposed in bed at 1123 K, (b)-(f) exposed above bed at (b) 1123 K, (c) 1073 K, (d) 923 K, (e) 823 K, and (f) 723 K. ANL Neg. No. 306-78-791

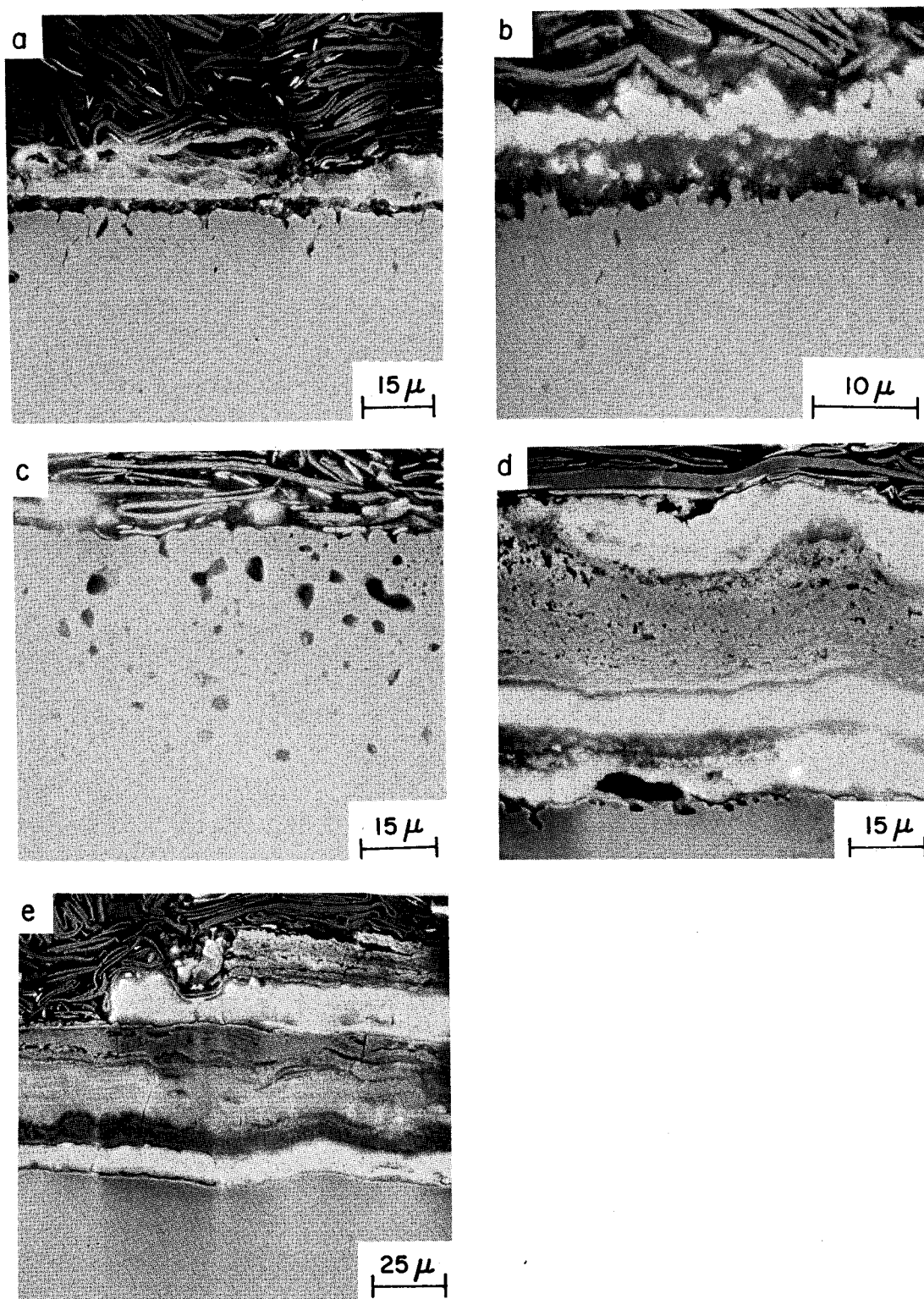


Fig. 21. SEMs of Type 310 Stainless Steel after a 100-h Exposure. (a) Exposed in bed at 1123 K, (b)-(e) exposed above bed at (b) 1123 K, (c) 1073 K, (d) 923 K, and (e) 823 K. ANL Neg. No. 306-78-792

The X-ray microprobe line analyses for iron, chromium, nickel, oxygen, and sulfur on Type 304 stainless steel specimens exposed at 650°C above the bed containing NaCl are shown in Fig. 22. The relative concentrations of these elements show that the outer surface scale consists mainly of iron and oxygen. The inner scale contains iron, chromium, and oxygen. The region below the oxides consists of nickel, iron, and sulfur. The X-ray images for the above elements and chlorine are shown in Fig. 23 along with a micrograph of the surface scale on the same specimen. The distribution of the various elements shows the two oxide layers and the region of internal sulfidation and oxidation. The X-ray image for chlorine shows that this element is present in regions which show a higher concentration of sulfur. This behavior was observed in all specimens exposed at 923 and 823 K. Chlorine was observed in the region between the oxide layer and the area of internal sulfidation. The sulfide/mixed-oxide and the mixed-oxide/iron-oxide interfaces observed in Type 304 stainless steel specimens exposed at 823 K are shown in Figs. 24a and 24b, respectively. Cubes of NaCl can be clearly seen in the sulfide region.

c. Conclusions

1. The addition of NaCl or CaCl_2 to the fluidized bed increases the corrosion rates.
2. In the presence of salt, Types 304, 316, and 310 stainless steel perform better than did the high-nickel alloys.
3. The corrosion behavior of stainless steels is relatively insensitive to the amount of NaCl in the bed.
4. The corrosion behavior of Inconel 600, Inconel 601, and RA 333 in the presence of 1.0 mol % NaCl or 0.1 mol % CaCl_2 is comparable to that of the stainless steels.
5. The internal corrosive attack consists of three distinct zones: internal oxidation, internal sulfidation, and a carburized zone where the carbon from the outer zone reprecipitates as chromium-rich carbides.
6. Specimens exposed above the fluidized bed at 923 and 823 K show extensive corrosive attack. In these specimens, chlorine was detected at the sulfide-oxide interface.

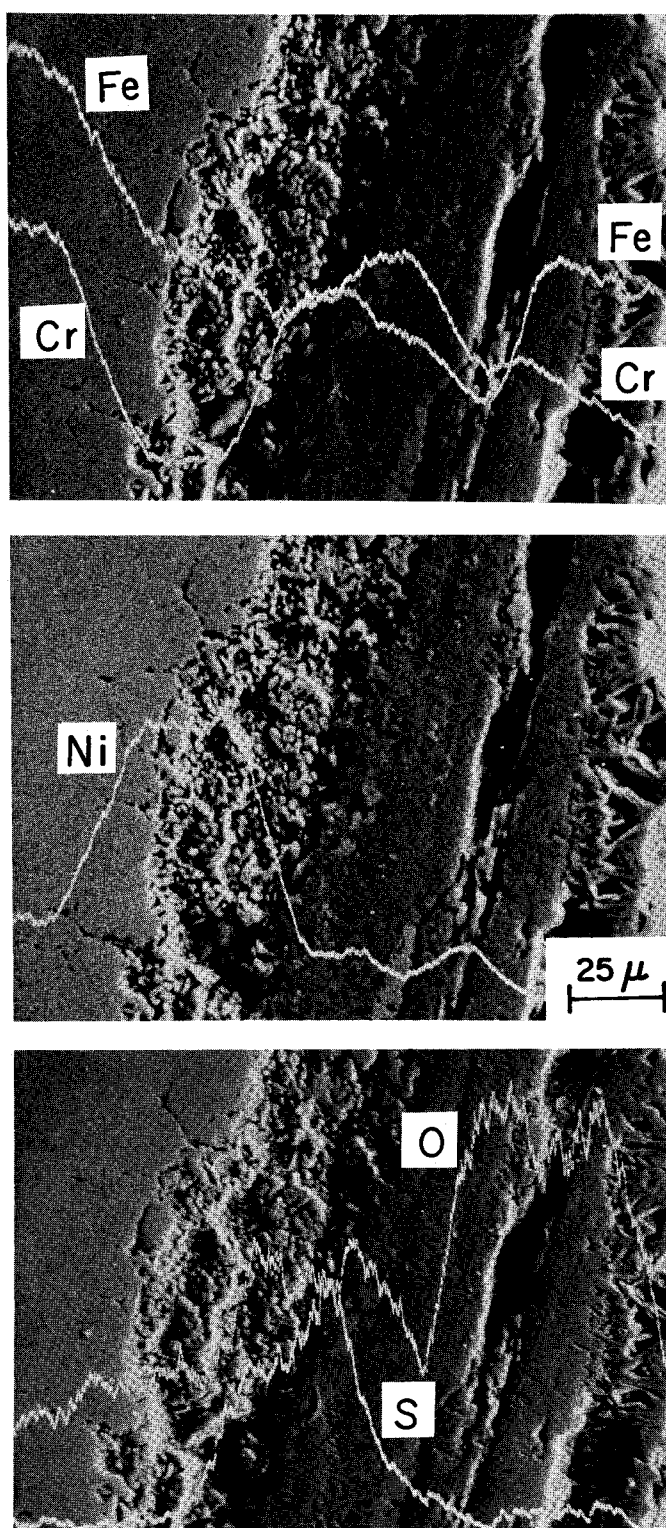


Fig. 22. X-ray Microprobe Line Analyses for Fe, Cr, Ni, O, and S on Type 304 Stainless Steel Specimen Exposed Above the Bed Containing NaCl for 100 h at 923 K. ANL Neg. No. 306-78-788

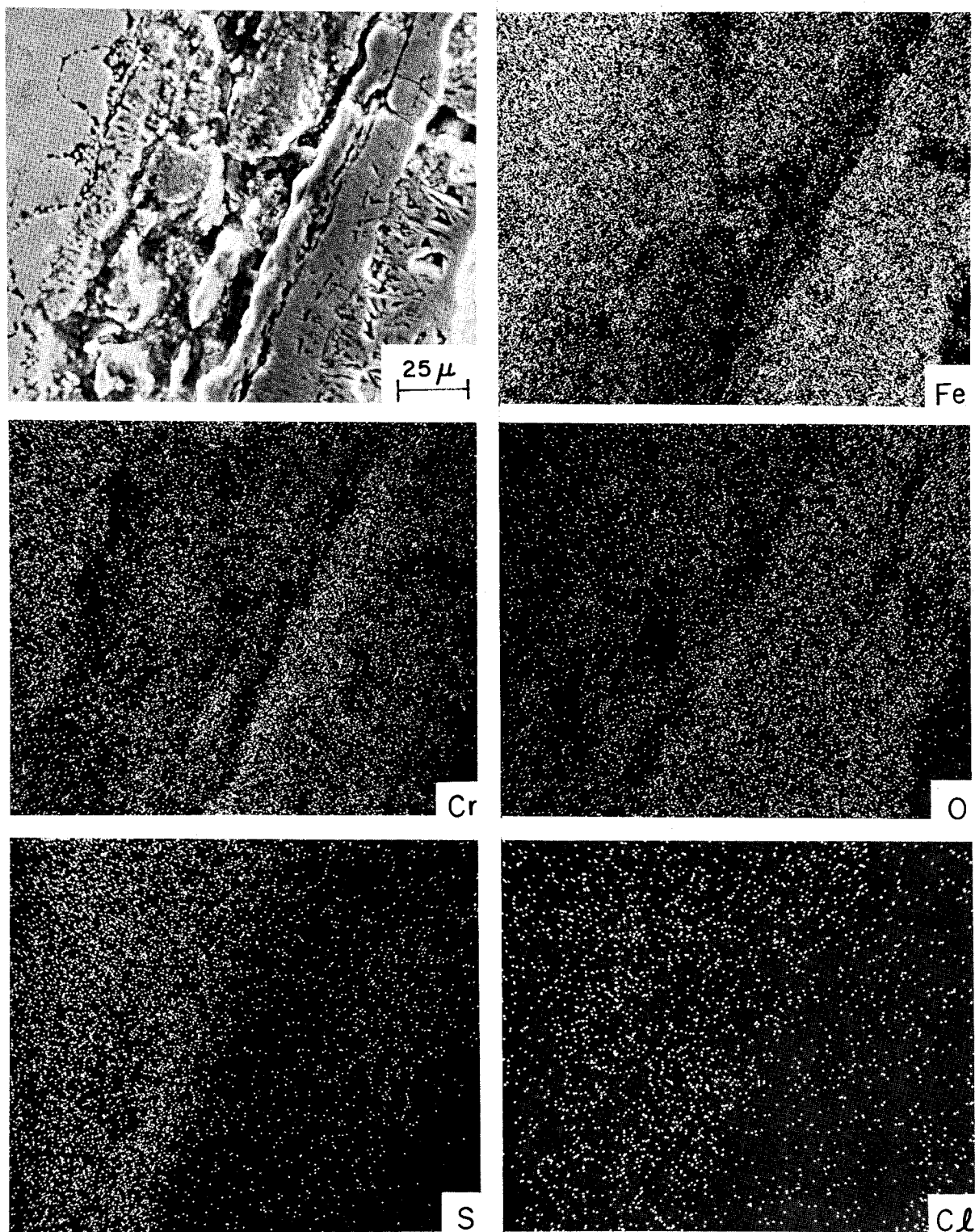


Fig. 23. SEMs and X-ray Images for Fe, Cr, O, S, and Cl of Type 304 Stainless Steel Specimen Exposed Above the Bed Containing NaCl for 100 h at 923 K. ANL Neg. No. 306-78-789

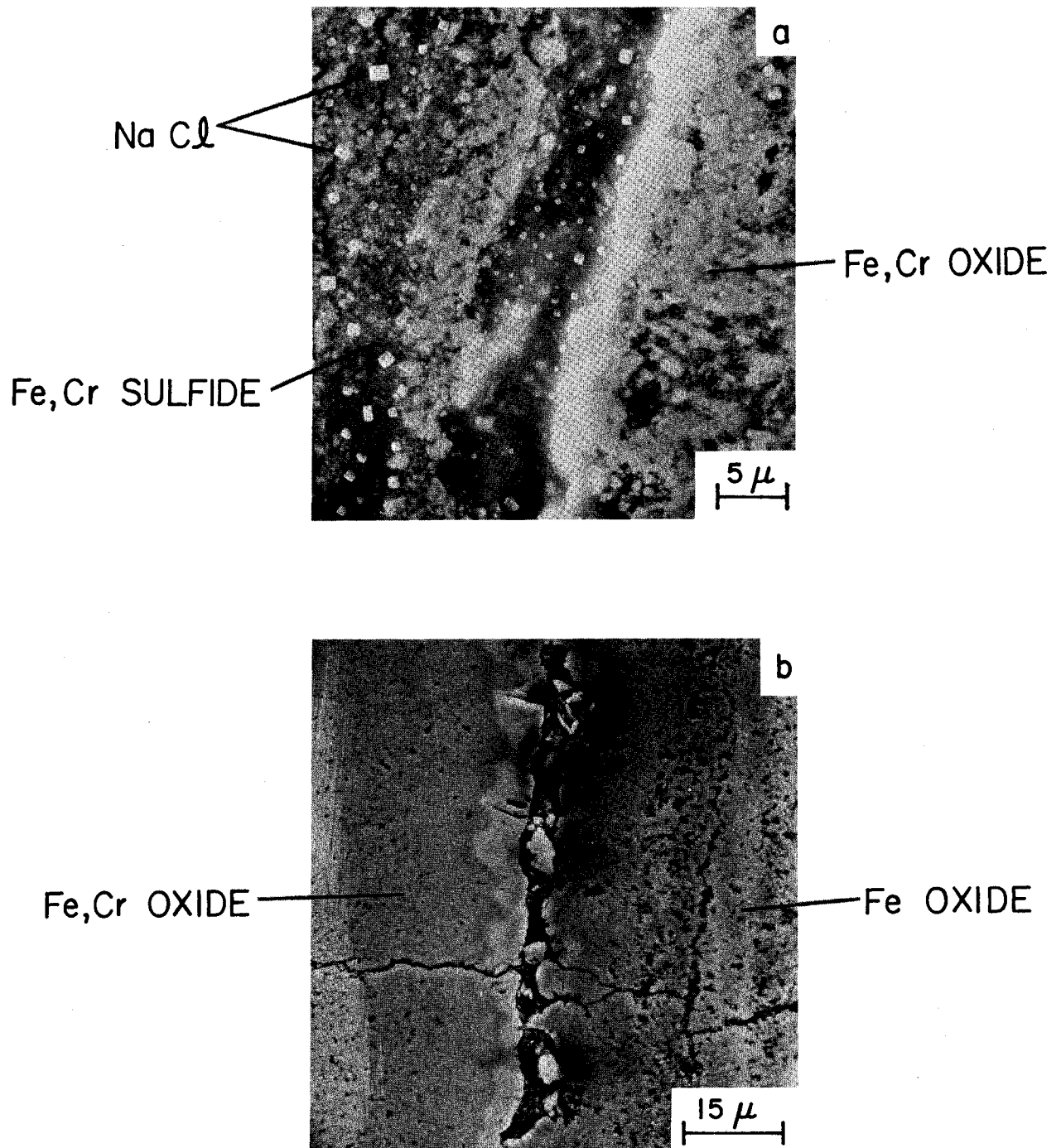


Fig. 24. SEMs of (a) Sulfide/Mixed-Oxide Interface and (b) Mixed-Oxide/Iron-Oxide Interface Observed in Type 304 Stainless Steel Specimen Exposed Above the Bed for 100 h at 823 K.
ANL Neg. No. 306-78-790

REFERENCES

1. G. J. Vogel et al., Supportive Studies in Fluidized-Bed Combustion, Quarterly Report, July-September 1977, Argonne National Laboratory Report, ANL/CEN/FE-77-8.
2. J. C. Montagna et al., Fluidized-Bed Regeneration of Sulfated Dolomite from a Coal-Fired FBC Process by Reductive Decomposition, Argonne National Laboratory Report, ANL-77-16 (April 1977).
3. G. J. Vogel et al., Supportive Studies in Fluidized-Bed Combustion, Annual Report, July 1976-June 1977, Argonne National Laboratory Report, ANL/CEN/FE-77-3.
4. G. J. Vogel et al., Regeneration of Sulfated Limestone from FBCs and Corrosive Effects of Sulfation Activators in FBCs, Quarterly Report, October-December 1977, Argonne National Laboratory Report, ANL/CEN/FE-77-10.
5. M. E. Whatley, A Dimensional Analysis of Solids Transport and Dispersion in a Rotary Kiln, Oak Ridge National Laboratory Report, ORNL/TM-5898 (July 1977).
6. J. Griswold, Fuels Combustion and Furnaces, McGraw Hill, New York, p. 421 (1946).
7. W. M. Swift et al., Decomposition of Calcium Sulfate: A Review of the Literature, Argonne National Laboratory Report, ANL-76-122, pp. 40-42 (December 1976).

TECHNICAL REPORT DATA (Please read Instructions on the reverse before completing)		
1. REPORT NO. EPA-600/7-79-157	2.	3. RECIPIENT'S ACCESSION NO.
4. TITLE AND SUBTITLE Regeneration of Sulfated Limestone from FBCs and Corrosive Effects of Sulfation Accelerators in FBCs: Annual Report		5. REPORT DATE July 1979
		6. PERFORMING ORGANIZATION CODE
7. AUTHOR(S) G. J. Vogel, I. Johnson, J. F. Lenc, D. S. Moulton, R. B. Snyder, J. A. Shearer, G. W. Smith, W. M. Swift, E. B. Smyk, F. G. Teats, C. B. Turner, and A. A. Jonke		8. PERFORMING ORGANIZATION REPORT NO. ANL/CEN/FE-78-13
9. PERFORMING ORGANIZATION NAME AND ADDRESS Argonne National Laboratory 9700 South Cass Avenue Argonne, Illinois 60439		10. PROGRAM ELEMENT NO. INE825
		11. CONTRACT/GRANT NO. IAG-D5-E681 (EPA) and W-31-109-Eng-38 (DOE)
12. SPONSORING AGENCY NAME AND ADDRESS EPA, Office of Research and Development* Industrial Environmental Research Laboratory Research Triangle Park, NC 27711		13. TYPE OF REPORT AND PERIOD COVERED Annual; 7/77 - 9/78
		14. SPONSORING AGENCY CODE EPA/600/13
15. SUPPLEMENTARY NOTES (*) Cosponsored by DOE. Project officers: D. A. Kirchgessner (EPA) and John Geffken (DOE).		
16. ABSTRACT The report gives 1977-78 results of studies supporting the national development of fluidized-bed combustion (FBC). Program objectives are to develop an economically/environmentally acceptable process for regenerating the partly sulfated product of the FBC of coal, to obtain the design data needed for the construction of larger regenerators, and to determine the corrosion of metallic alloys by sulfation acceleration agents added to the limestone sorbent. A regeneration process model has been developed and used to investigate the effects of the main variables on regenerator size and performance and to estimate the economic feasibility of regeneration. It reports results of an investigation of a regeneration process using a rotary kiln in place of FBC. An atmospheric pressure FBC was operated to study the corrosion of metallic alloys by limestone treated with various sulfation accelerators (e.g., NaCl and CaCl ₂). It gives results of laboratory scale corrosion studies.		
17. KEY WORDS AND DOCUMENT ANALYSIS		
a. DESCRIPTORS	b. IDENTIFIERS/OPEN ENDED TERMS	c. COSATI Field/Group
Pollution	Desulfurization	Pollution Control
Fluidized Bed Processing		Stationary Sources
Calcium Chlorides	Dolomite	Atmospheric Fluidized
Combustion	Inconel	Bed Combustor
Coal	Automation	Incoloy 800
Additives	Accelerating Agents	Metal Sulfidation
Sulfur Oxides	Limestone	
18. DISTRIBUTION STATEMENT Release to Public		19. SECURITY CLASS (This Report) Unclassified
		20. SECURITY CLASS (This page) Unclassified
		21. NO. OF PAGES 63
		22. PRICE